



**TRIBHUVAN UNIVERSITY
INSTITUTE OF ENGINEERING
PULCHOWK CAMPUS**

Thesis no: M-78-MSMDE-2021-2023

**Study of the Effects of Blockage and Impeller Fault in Centrifugal Pump using
CFD Simulation**

by

Bibek Adhikari

A THESIS SUBMITTED TO THE DEPARTMENT OF MECHANICAL AND
AEROSPACE ENGINEERING IN PARTIAL FULFILLMENT OF THE
REQUIREMENTS FOR THE DEGREE OF MASTERS OF SCIENCE IN
MECHANICAL SYSTEMS DESIGN AND ENGINEERING

DEPARTMENT OF MECHANICAL AND AEROSPACE ENGINEERING
LALITPUR, NEPAL

NOVEMBER, 2023

COPYRIGHT

The author has agreed that the library, Department of Mechanical and Aerospace Engineering, Pulchowk Campus, Institute of Engineering may make this thesis freely available for inspection. Moreover, the author has agreed that permission for extensive copying of this thesis for scholarly purpose may be granted by the professor(s) who supervised the work recorded herein or, in their absence, by the Head of the Department wherein the thesis was done. It is understood that the recognition will be given to the author of this thesis and to the Department of Mechanical Engineering, Pulchowk Campus, Institute of Engineering in any use of the material of this thesis. Copying or publication or the other use of this thesis for financial gain without approval of the Department of Mechanical and Aerospace Engineering, Pulchowk Campus, Institute of Engineering and author's written permission is prohibited.

Request for permission to copy or to make any other use of the material in this thesis in whole or in part should be addressed to:

Head

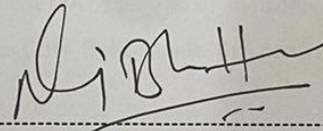
Department of Mechanical and Aerospace Engineering

Pulchowk Campus, Institute of Engineering

Lalitpur, Kathmandu

**TRIBHUVAN UNIVERSITY
INSTITUTE OF ENGINEERING
PULCHOWK CAMPUS
DEPARTMENT OF MECHANICAL AND AEROSPACE ENGINEERING**

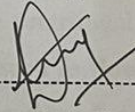
The undersigned hereby certify that they have read, and recommended to the Institute of Engineering for acceptance, thesis entitled “**Study of the Effects of Blockage and Impeller Fault in Centrifugal Pump using CFD Simulation**” submitted by **Bibek Adhikari (PUL078MSMDE005)** in partial fulfillment of the requirements for the degree of Master of Science, Mechanical Systems Design and Engineering.



Supervisor, Nawraj Bhattarai, Ph.D.

Associate Professor

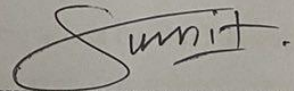
Department of Mechanical and Aerospace Engineering



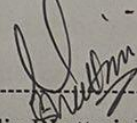
Supervisor, Kamal Darlami

Assistant Professor

Department of Mechanical and Aerospace Engineering



External Examiner, Er. Sumit Maharjan



Committee Chairman, Sudip Bhattarai, Ph.D.

Head of Department

Department of Mechanical and Aerospace Engineering



2023/11/26

Date

ABSTRACT

Centrifugal pumps have been used as a vital component in most of the industrial applications aiding the way for liquid transport in various sectors ranging from the construction, manufacturing, hydropower, wastewater treatments to petrochemicals. The efficient and reliable operation of these pumps is very much crucial for any industry. However, the pumps are prone to various faults and defects during their life cycle which arises the necessity for addressing certain diagnostic tools for early fault detections and preventions. For these pumps to operate efficiently, it is very much important to understand the intricate dynamics inside the pump. This paper investigates the use of the open-source software OpenFOAM as one of the tools used in Computational Fluid Dynamics for studying the flow field inside the centrifugal pump.

Steady-state simulations are performed using the simpleFoam solver via the MRF approach while the unsteady transient simulations are performed using pimpleFoam solver via the Sliding Mesh approach. A CFD model of Oberdorfer 60P pump have been developed to simulate the fluid flow pattern inside the centrifugal pump. The study mainly focuses on assessing critical pump parameters such as flow rate, head, pressure distribution, forces and torques characteristics. The flow field inside the pump are visualized using the ParaView utility of the OpenFOAM. The velocity vectors, static pressure across the domain is plotted and shown. The presence of blockage in the centrifugal pump results in the decrement of the static pressure near the inlet region thus increasing the change in static pressure across the fluid domain. The maximum flow velocity near the outlet section of the pipe gets reduced which results in the decrement of the discharge at the outlet. The presence of crack reduces the static pressure in overall domain. With increase in crack depth the static pressure decreases risking to the occurrence of cavitations. These results conclude that monitoring variation in pump parameters such as flow velocity and static pressure in the pump domain helps in developing an efficient methodology for fault detection and diagnosis system.

ACKNOWLEDGEMENT

I would like to express my sincere gratitude to my supervisors Associate Prof. Dr. Nawraj Bhattraï and Assistant Prof. Kamal Darlami, Pulchowk Campus for their valuable guidance while doing the thesis. Without their continuous support and guidance, this research would not have been completed.

I would like to express my deepest appreciation to Assistant Prof. Dr. Sudip Bhattraï, Head of Department, Department of Mechanical and Aerospace Engineering for his invaluable support throughout the thesis duration.

I would like to express sincere gratitude to Professor Dr. Laxman Poudel, Coordinator, M.Sc. in Mechanical Systems Design and Engineering. My special thanks to the entire family of the Department of Mechanical and Aerospace Engineering for the constant support and coordination. I am grateful for the valuable suggestions and kind support which I received from all the teachers and faculty members of the department during the time of my research. I am grateful for the valuable suggestions and kind support which I received from all the teachers and faculty members of the department during the time of my research.

I would like to express my special thanks of gratitude to Professor Dr. Rajiv Tiwari, IIT, Guwahati and his team for generously providing the experimental data used in this study. I am grateful for their collaboration and the valuable insights they provided.

I express my thanks to Er. Sunil Sharma, Er. Anup Pandey, Er. Sanjeev Adhikari, Er. Amrit Tiwari, Er. Abhishek Bhandari, Er. Akin Chhetri, Er. Sandip Gewali, Er. Bijay Galami for their invaluable insights during this work. I would like to thank Er. Nishan Timilsina, Mr. Saugat Paudel for their support and encouragement during the time of this thesis work.

I appreciate everyone who has supported me in any form with this thesis work.

TABLE OF CONTENTS

COPYRIGHT.....	ii
ABSTRACT.....	iv
ACKNOWLEDGEMENT.....	v
LIST OF FIGURES.....	viii
LIST OF TABLES.....	x
LIST OF ABBREVIATIONS.....	xi
CHAPTER ONE: INTRODUCTION.....	1
1.1 Background.....	1
1.2 Statement of the Problem.....	3
1.3 Rationale.....	4
1.4 Objective of the Research.....	5
1.4.1 Main Objective.....	5
1.4.2 Specific Objectives.....	5
1.5 Limitations of the Research.....	5
1.6 Testcase Description.....	6
CHAPTER TWO: LITERATURE REVIEW.....	7
2.1 CFD for Centrifugal Pump.....	7
2.2 Fault diagnosis of Centrifugal Pump.....	8
2.3 Flow Blockage in Centrifugal Pump.....	10
2.4 Centrifugal Pump Fault Simulation Test Setup.....	11
2.5 Blockage Modeling in the Experiment.....	12
2.6 Softwares.....	14
2.6.1 ANSYS Meshing.....	14
2.3.2 OpenFOAM.....	14
2.7 Steady-State Solver: SimpleFoam.....	15

2.8 Unsteady-State Solver: PimpleFoam	16
CHAPTER THREE: METHODOLOGY AND DESIGN STUDY	18
3.1 Conceptual Framework.....	18
3.2 Literature Review.....	19
3.3 Design Study	21
3.3.1 Geometry Modeling and Mesh Creation.....	21
3.3.3 Solvers and Case Setup.....	27
3.3.2 Grid Independence Test	29
CHAPTER FOUR: RESULTS AND DISCUSSION	31
5.1 Simulation Results Validation	31
5.1.1 Result Validation with Pump Performance Chart.....	31
5.1.2 Result Comparison with the Experimental Data.....	33
5.2 Simulation Results on the Blockage	38
5.2.1 Pump Flow Development	38
5.2.2 Pressure Distribution.....	40
5.2.3 Flow Field Velocity Vectors	40
5.2.4 Static Pressure and Flow Velocity with Blockage	41
5.3 Simulation Results on the Impeller Crack	43
CHAPTER FIVE: CONCLUSIONS AND RECOMMENDATIONS	47
5.1 Conclusions.....	47
5.2 Recommendations.....	48
REFERENCES	49
APPENDIX.....	51

LIST OF FIGURES

Figure 1: Rendered Image of the Pump	2
Figure 2: Geometry of the Pump 60P-Oberdorfer	6
Figure 3: Experimental Setup used in Kumar et.al (2021)	11
Figure 4: Location of the Pressure Transducers	12
Figure 5: Pump with Impeller Crack used by Rapur et. al (2016).....	12
Figure 6: (a) Mechanical Valve, (b) Blockage Positions	13
Figure 7: Flowchart for Research Methodology	18
Figure 8: Coordinate Position of the Pressure Sensors used in Simulation.....	20
Figure 9: CAD Model of Oberdorfer 60P Pump	21
Figure 10: Exploded View of the Oberdorfer 60P Pump	21
Figure 11: Computational Fluid Domain with Exploded View.....	22
Figure 12: Structured Mesh used in the Inlet Domain.....	23
Figure 13: Mesh Showing Inflation Layer used in the Inlet Domain	24
Figure 14: Mesh used in Impeller Rotor Domain	24
Figure 15: Surface Mesh used in the Impeller Blades	25
Figure 16: Mesh used in the Volute Domain	25
Figure 17: Impeller Crack.....	26
Figure 18: Mesh used in the Impeller with Faults	26
Figure 19: Basic OpenFOAM case Structure	27
Figure 20: Grid Independence Test.....	29
Figure 21: Result validation at 0.5LPS	31
Figure 22: Result validation at 3000 RPM	32
Figure 23: Result validation at 3000 RPM	33
Figure 24: Experimental Validation of the Simulation.....	33
Figure 25: Pressure Signal with Time - Experimental.....	34

Figure 26: FFT of the Pressure Signal at Probe-1 – Experimental	34
Figure 27: Pressure Signal with Time – 1800 RPM	35
Figure 28: FFT of the Pressure signal at Probe 1 – 1800 RPM.....	35
Figure 29: FFT of the Pressure signal at Probe 2 – 1800 RPM.....	36
Figure 30: Pressure Signal with Time – 3000 RPM	36
Figure 31: FFT of the Pressure signal at Probe 1 – 3000 RPM.....	37
Figure 32: FFT of the Pressure signal at Probe 2 – 3000 RPM.....	37
Figure 33: Flow Develop inside the Pump (steady-state).....	38
Figure 34: Developed Flow at Inlet Section	39
Figure 35: Flow at Outlet Pipe.....	39
Figure 36: Static Pressure Distribution in the pump (steady-state) left: 0.504 LPS, mid: 0.63 LPS, right: 0.757 LPS.....	40
Figure 37: Velocity Vectors in the pump (steady-state) left: 0.504 LPS, mid: 0.63 LPS, right: 0.757 LPS	41
Figure 38: Static Pressure Variation with Blockage	42
Figure 39: Mag (U_y) Variation with Blockage	43
Figure 40 : Impeller Fault with crack at the top on the blades	43
Figure 41: Static Pressure values with time	45
Figure 42: FFT-4mm crack.....	45
Figure 43: FFT-4.2mm crack.....	46
Figure 44: FFT-4.4mm crack.....	46

LIST OF TABLES

Table 1: Feature and Design Parameter of the Oberdorfer 60P Pump	6
Table 2: Number of Elements for each domain	22
Table 3: Initial values and Boundary Conditions used in the Simulation.....	28
Table 4: Study of pump performance with Blockage level	41
Table 5: Variation of Static Pressure with Crack Depth.....	44

LIST OF ABBREVIATIONS

CFD	Computational Fluid Dynamics
FEA	Finite Element Analysis
openFOAM	Open-source Field Operation and Manipulation
ANSYS	Analysis System
CP	Centrifugal Pump
RPM	Rotation Per Minute:
LPS	Liter Per Second
GPM	Gallon Per Minute
RANS	Reynolds Averaged Navier-Stokes
URANS	Unsteady Reynolds Averaged Navier-Stokes
SST	Shear Stress Transport
FFT	Fast Fourier Transform
SIMPLE	Semi Implicit Method for Pressure Linked Equations
SIMPLEC	Semi Implicit Method for Pressure Linked Equations Consistent
PISO	Pressure Implicit Split Operator
PIMPLE	PISO + SIMPLE
MRF	Multiple Reference Frame
CAD	Computer Aided Design
AMI	Arbitrary Mesh Interface

CHAPTER ONE: INTRODUCTION

"Pumps" are hydraulic devices that transform mechanical energy into hydraulic energy in the form of pressure energy. The hydraulic device is referred to as a "centrifugal pump" if the fluid's centrifugal force is used to transform mechanical energy into pressure energy.

Centrifugal pumps are designed to increase the fluid pressure. Centrifugal pumps are rotary devices with two main components: an impeller and a volute casing. The impeller is the rotary component which consists of a series of curved blades while the volute casing is the static component. In principle, the centrifugal pumps use a rotating impeller to give rotation to the fluid developing dynamic pressure which enable the lifting of the fluids from the lower level to a higher level. The liquid enters the pump through the eye of the impeller and is pushed by the impeller radially into the volute

1.1 Background

Centrifugal pumps play an important role in many of the engineering applications. They are most commonly used in different fields of engineering such as industries, agriculture and domestic applications. Centrifugal pumps are preferred over other types of pumps because they are relatively simple to design, easy to install and maintain, and also are highly efficient at transferring fluids. They can handle a wide range of pressures and flow rates. They are often used to lift liquids such as water, chemicals, oils and other fluids from one place to other. However, they are not suitable for handling viscous or fluids with high solid content. The design of the centrifugal pump involves several key components including the impeller, casing, inlet and outlet ports, and shaft. The pump performance is determined by several key factors including its design, operating conditions and the characteristics of the liquid being used. The key pump performance parameters are pressure head, flow rate and efficiency. The input power P required while pumping a fluid of density ρ to a height H at a flow rate of Q is given by the following formula:

$$P = \frac{\rho g Q H}{\eta} \quad (1.1)$$

Where, η = efficiency of the pump, g = acceleration due to gravity.

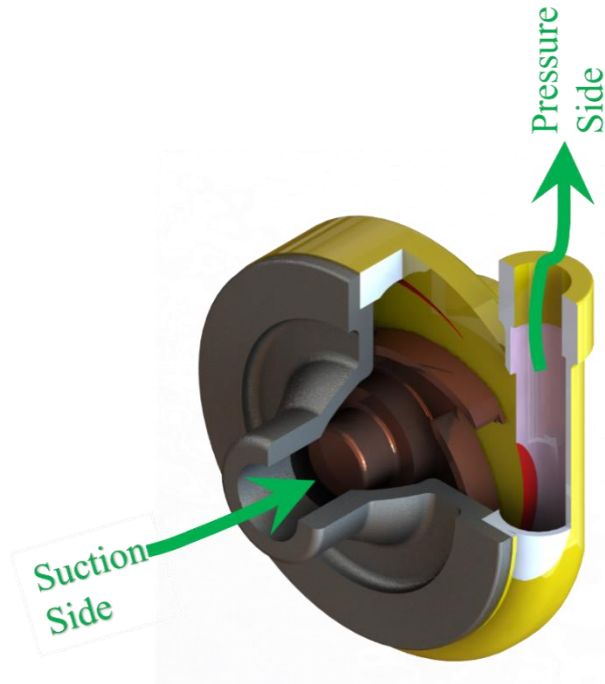


Figure 1: Rendered Image of the Pump

The Figure 1 shows the image of a centrifugal pump with suction and pressure side indicated. For different flow rate, the input power required while pumping the fluid gets different. i.e., for smaller value of Q , smaller is the input power required. Similarly, for same input power, the pressure head and discharge are inversely proportional. When the total pressure difference Δp across the outlet and the inlet patch is known, the head can be calculated as:

$$H = \frac{\Delta p}{\rho g} \quad (1.2)$$

Centrifugal pumps are prevalent for many different applications in the engineering world and it is being used from the time prior of the industrial revolution. In 1687 A.D., the first true centrifugal pump was developed by a French inventor Denis Papin (Yannopoulos, et al., 2015). The design was simple consisting of a straight vane impeller and casing with a spiral volute used for local drainage. However, the centrifugal pump as we know in the present was designed and developed in the mid of the 19th century. These modern pumps featured improvements in the design of the impeller, shape of the casing and the sealing used which resulted in the improvement of the performance and the efficiency of the pump. Since then, centrifugal pumps have gone under numerous design improvements. Numerous researches have been

done for studying the design and performance parameters. Nevertheless, their design and performance prediction study are still a difficult task to make, mainly due to the large number of the design parameters involved. Also, the cost and time for studying the design and performance of the pump by constructing and testing the physical models is high. And for this reason, Computational Fluid Dynamics (CFD) analysis is being predominantly used to study the design and performance parameters of the centrifugal pumps. The use of CFD in centrifugal pump design is becoming more and more prevalent due to advancements in computational power, the ease with which 3D geometry can be created, and the potent visualization tools available. CFD is an essential tool for cutting design process costs and times.

The fluid flow inside a healthy centrifugal pump is complex and hard to predict mainly due to the large number of the complex geometrical parameters involved. The presence of any defect inside the pump will then make the fluid flow more complex and very hard to predict. Research have been made to study the fluid flow and performance of a centrifugal pump with defects. Impeller cracks, Inlet and outlet blockage defects, presence of impurities, Pitted cover plate faults, cavitation, bearing faults, misalignments are some of the faults in a centrifugal pump. Both independent and compound defects can exist inside the centrifugal pump. In presence of such defects, it is very time consuming and expensive to physically build and test the fluid flow and the performance of the centrifugal pump. Therefore, the only method for understanding the operation of a centrifugal pump with defects is to utilize CFD to simulate the fluid flow.

1.2 Statement of the Problem

Model and Prototype testing of a centrifugal pump is a difficult, time consuming and expensive task. The design and performance study of a centrifugal pump is a complex process. It is difficult to perceive and visualize the fluid flow inside the pump. When a centrifugal pump has an issue, the fluid flow becomes significantly more complicated, making it difficult to predict the way the pump will work. Anticipating the performance of pumps before they are manufactured is essential for their efficient and economical design. Understanding the behavior of fluid flow in the various region of pump is necessary for this. One approach for understanding fluid flow and foresee

the pump performance is by experimental model testing, however this method is expensive, tedious, and time-consuming (Shah, Jain, Patel, & Lakhera, 2013). CFD has recently become essential for understanding fluid flow behavior and predicting centrifugal pump performance.

CFD analysis is being predominantly applied in the design of the centrifugal pump. With the aid of this tool, the complex fluid flow inside the pump can be well predicted and understood. This helps to speed up the design procedure by simply skipping the tedious task of physical model and prototype testing. Understanding the fluid flow of a centrifugal pump with defects through physical model creation is an expensive and time-consuming process. However, CFD analysis of such pumps can easily be done by changing the geometry and design parameters. The results from the analysis can then be directly compared with the known experimental data for validating. Thus, the use of CFD is more economical and less time consuming than experimental model testing.

In addition, numerous studies on the design and performance of the centrifugal pump have been done by changing the geometry such as shape of the volute, impeller shape, number of blades, types of blades, etc. and also by changing the design parameters such as inlet condition, pressure head required, rotational speed, etc. Therefore, CFD can be used to study the fluid flow behavior inside the centrifugal pump for such cases.

1.3 Rationale

The basis of this research thesis is to increase our understanding on the impacts of fault presence on fluid flow behavior inside the centrifugal pump. The primary emphasis lies on the study of fluid behavior due to the introduction of blockage at the inlet pipe. This study also aims to compare the results obtained from the CFD simulation and the experimental data available for different blockage level at the inlet pipe.

1.4 Objective of the Research

1.4.1 Main Objective

The main objective of this thesis is to study the fluid flow behavior inside a centrifugal pump with and without any faults such as blockage and impeller crack.

1.4.2 Specific Objectives

- To develop a CFD model of a centrifugal pump with and without any faults.
- To perform a CFD simulation of an existing centrifugal pump with and without any faults.
- To quantify the impact of faults on pump performance parameters with the help of baseline simulation.
- To help develop a fault detection and diagnosis system for centrifugal pumps based on CFD simulation data.

1.5 Limitations of the Research

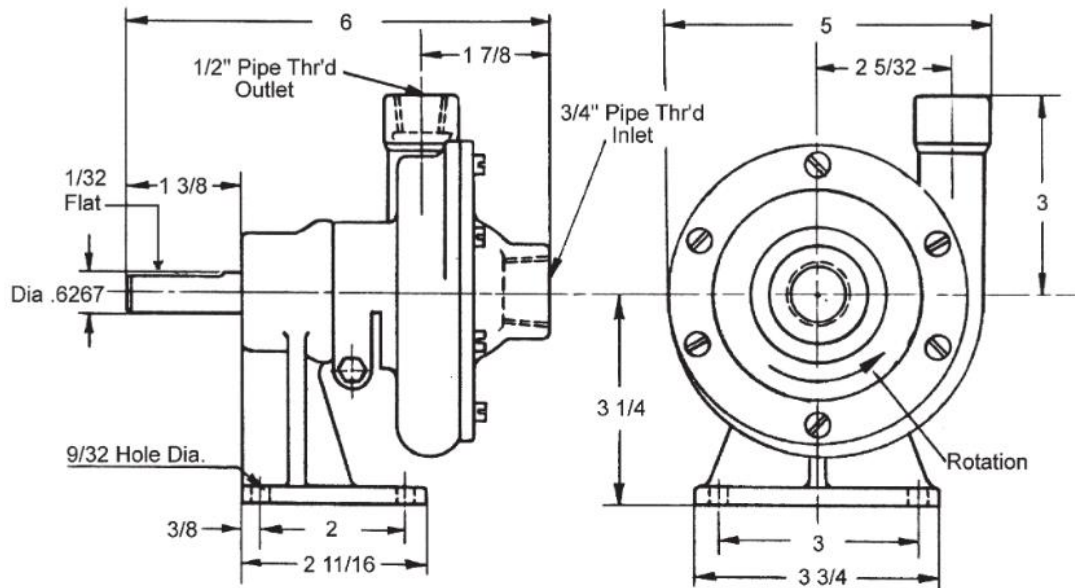
- 1 The study does not focus on the study of the cavitation.
- 2 The study is limited to numerical simulation.
- 3 It is assumed that the pump inlet is horizontal and the outlet is vertical.
- 4 Limited experimental data.

1.6 Testcase Description

As seen in the Figure 2, the 60P Oberdorfer centrifugal pump has been selected for the study. The pump consists of an impeller with an outer diameter of 90mm and 5 backward curved blades. The pump characteristics and design specifications are as follows:

Table 1: Feature and Design Parameter of the Oberdorfer 60P Pump

Rotational speed	1725 to 3450 RPM
Ports	Inlet: 23mm, Outlet: 18mm
Flow	Up to 24 GPM (1.5 LPS)
Head	Maximum 53 ft. (16 m)
Temperature	20° C
Number of Blades	5



[Source: pumpvendor.com/Oberdorfer_60P_series.html]

Figure 2: Geometry of the Pump 60P-Oberdorfer

CHAPTER TWO: LITERATURE REVIEW

Centrifugal pumps find widespread use in domestic, agricultural, and many production plant applications. They frequently have a major impact on keeping the plant flow intact. The process flow in the plants may partially or completely stop as a result of their failure. The presence of impurities, blockage, impeller defects, faulty installation, cavitation are one of the major faults likely to happen in a centrifugal pump. Centrifugal pumps are prone to a variety of common flaws, including those that are mechanical (bearing faults, misalignments, seal defects, and impeller defects), systemic (faulty installation and setup, obstruction and leakage), operational (cavitation, flow instabilities), or the combination of these.

Pump failures lead to changes in operation that lower efficiency or may cause the pump to break down. McKee et al. (2011) have identified and categorized the many pump failure types that are present in centrifugal pumps.

2.1 CFD for Centrifugal Pump

Typically, a CFD examination of an issue begins with the following actions:

- The Problem Definition
- Mathematical Modeling
- Pre-processing and Mesh Generation
- Solving
- Post-processing
- Verification and Validation

The objective for conducting any CFD analysis is to gain a more profound understanding of the physical phenomenon being studied. Since, simulation results are often compared and validated with experimental data, it is crucial to understand the process that are being done while performing the analysis. In order to run the simulation successfully, the physical process must be properly modeled, the flow domain needs to be discretized efficiently and the boundary conditions should be implemented correctly. As for the research, the CFD analysis is done for a centrifugal pump. Since fluid transportation uses centrifugal pumps extensively. Pump engineers are frequently asked to produce pumps that are more efficient, quiet, reliable and cost effective. Many studies have been made to study about the behavior of the fluid flow and performance prediction of the pump. Shah et. al (2013) in his paper reviewed the

state-of-the-art in CFD for centrifugal pumps. The CFD technique has been widely applied to centrifugal pumps as a numerical simulation tool for parametric study, cavitation investigation, and performance prediction at design and off-design circumstances. URANS turbulence model together with two equation k and ϵ were found to be reliable for accurate estimation of the pump performance parameters.

Commercial and open-source program for example ANSYS, OpenFOAM, etc. are used for the numerical simulation of the centrifugal pump. The number of blades, turbulence model employed, wrap angle, blade angles and all other factors can affect how well a centrifugal pump performs. According to Jaiswal (2014), when discharge rises the head falls, power input rises, and pump efficiency rises. Compared to other turbulence models, the SST turbulence model yields superior results.

The direct and inverse methods of centrifugal pump design were examined by Lei et al. (2014). While increasing the centrifugal pump's performance, most research focuses on parameter optimization and design methodology. This study demonstrates how the blade wrap angle is a critical design component that significantly affects pump performance. The investigation of the impact of the blade wrap angle on centrifugal pump performance presented in this study may help with centrifugal pump optimization.

2.2 Fault diagnosis of Centrifugal Pump

Centrifugal pumps are crucial for the smooth operation of many industries and plants. However, they can fail due to mechanical or hydraulic issues which by the way sometimes can coexist in the pump. Machine learning techniques for vibration-based conditional monitoring are frequently employed for pump malfunction diagnosis and detection. More significant issues with a centrifugal pump include noise, leakage, vibration, and defects on the impeller, seal, bearing, and cavitation. Further unfavorable consequences of cavitation include erosion, shaking of the structure, and deterioration of the hydraulic performance, which includes a decrease in head capacity and efficiency. Sakthivel (2009) described the use of decision trees for vibration-based defect diagnostics of a mono-block centrifugal pump. The following classical states—bearing fault, impeller fault, seal fault, impeller and bearing fault combined, and cavitation—are shown in the study based on simulation findings. One

defect at a time was introduced, and vibration signals and the pump's performance characteristics were recorded.

In terms of condition monitoring, fault identification and isolation were first presented by A.R. Mohanty et al. (2012) in their work. Although condition monitoring cannot stop failure, it can foresee it by measuring specific factors. Self- diagnostic capability of a pump refers to the pump's ability to automatically identify and diagnose problems within itself. The addition of this capability improves the reliability and reduce the need for human intervention. When a centrifugal pump has self-diagnostic capability, it can monitor its own performance and identify any issues that may arise. This work uses the motor current signature analysis and FFT of the vibration signals to approach self-diagnostic capability. As the impeller defect gets worse, the vibration signal's peak value gets higher.

When the design of the pump does not properly accommodate the flow conditions, it can lead to several issues, including flow separation, recirculation, and vortex formation. These problems can result in pump performance deterioration and operational inefficiencies. In their research, Rapur et al. (2017) outlines suction obstruction and impeller flaws as two of the main sources of flow instabilities. The paper attempts to categorize these errors. Using the radial basis function (RBF) kernel and support vector machine (SVM) technique, tri-axial vibration data from the pump are used to categorize the defects. The work is notable for using Support Vector Machines (SVM) to categorize both distinct and concurrent problems. The research may help the industry forecast how to assess the degree of obstruction and impeller flaws in centrifugal pumps.

The classification of different defects that can arise in a centrifugal pump at known and unknown test speeds is the main emphasis of Rapur et al. (2019). Both co-occurring and independently existing flaws are taken into account in this work. Principal component analysis (PCA) and wavelet packet transform (WPT) decomposition are the two classification approaches that are suggested. It is discovered that a classifier trained with vibration and motor current data works better than one learned with just one feature alone.

Tiwari et al. (2020) investigated a fluid pressure-based approach to determine the existence and the degree of blockages and cavitation in centrifugal pumps. To

simulate blockages, the suction pipe's flow area is reduced at various levels, and pressure readings are taken for various operating speeds using a pressure transducer. The pressure transducer data is classified using a deep learning system. The study discovered that at greater speeds and blockage levels, cavitation becomes more prevalent. The suggested methodology, according to the paper, can be used to accurately identify cavitation and blockage defects in centrifugal pumps.

The diagnosis of a blockage defect in the centrifugal pump's input pipe utilizing data from various sensor types, including an accelerometer, pressure transducer, and motor line current probe, is covered by Kumar et al. (2021). The study uses a deep learning algorithm for multiclass classification as its methodology. The study emphasizes the value of gathering data from multiple sources, and the findings demonstrate that combining various sensor data types increases the precision of determining the blockage level. The findings demonstrate that pressure data can be utilized to determine the degree of obstruction, however pressure sensors produce predictions with less accuracy than other types of sensors. All things considered, the report offers insightful information about the application of various data for centrifugal pump failure diagnostics and detection. The results can be used to create fault detection and diagnostic techniques for any system that are more precise and dependable, which can increase cost-effectiveness, safety, and efficiency.

The following is a list of the various defect types that can affect centrifugal pumps:

1. Mechanically Developed: Misalignment; bearing faults, seal defects, impeller defects
2. System Development: Inadequate installation; blocking and seeping
3. Developed Operationally: Cavitation and flow instabilities

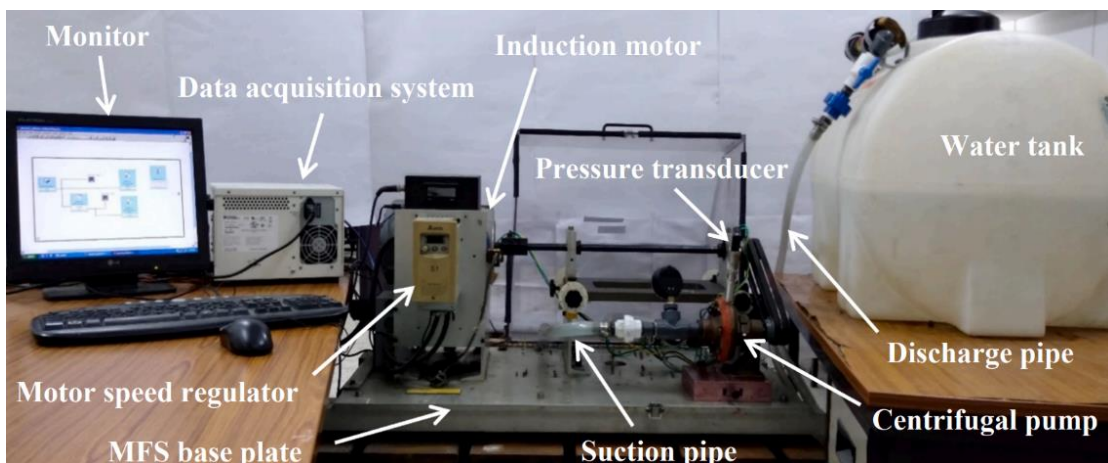
2.3 Flow Blockage in Centrifugal Pump

The presence of blockage in centrifugal pump whether upstream of the inlet pipe or the downstream of the outlet pipe risks the reliability of its operation. These blockages when present leads to the reduction in the pump's flow rate, possibility of cavitations, overheating of pump components or mechanical parts breakdown which would eventually increase the cost for maintenance. Blockage in the pump occurs due to the deposition of organic matter at the pump inlet, outlet or any other areas inside the channels. The flow blockage in the suction pipe will cause restriction in the flow of the fluid which leads to the lower static pressure distribution inside the pump.

Pressure transducers at the different sections of the pump can be used to monitor the static pressure distribution inside the pump. Furthermore, presence of blockage in the pump will result in excessive vibration of the impeller and noise.

2.4 Centrifugal Pump Fault Simulation Test Setup

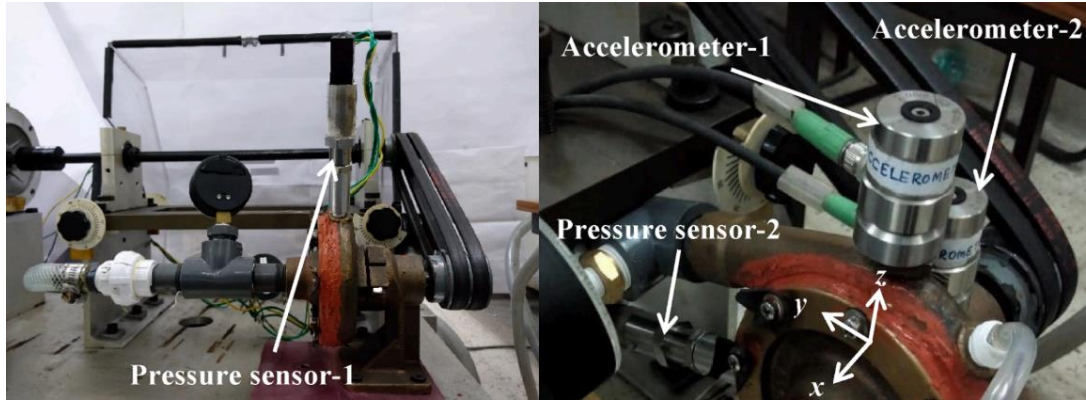
This research is based on the papers by Kumar et. al (2021) titled “Identification of inlet pipe blockage level in centrifugal pump over a range of speeds by deep learning algorithm using multi-source data” and Rapur et. al (2016) titled “Experimental Time-Domain Vibration Based Fault Diagnosis of Centrifugal Pumps Using Support Vector Machine”. In both the paper, faults such as blockage and impeller cracks in centrifugal pump are studied. This research focuses on creating a CFD simulation based on the experimental setup from the above-mentioned paper. The simulation results are compared and validated with the experimental data from these papers. The Figure 3 shows the experimental setup used by Kumar et. al (2021).



(Kumar, Dewangan, Tiwari, & Bordoloi, 2021)

Figure 3: Experimental Setup used in Kumar et.al (2021)

The Figure 4 shows the location of the two-pressure probe used in the experiment.



(Kumar, Dewangan, Tiwari, & Bordoloi, 2021)

Figure 4: Location of the Pressure Transducers

Figure 5 shows the Oberdorfer 60P pump with impeller crack used by Rapur et. al (2016). In their research two geometrically similar pump are used. One of the pumps is healthy and in the other one, two through-through rectangular shaped artificial cracks per impeller vane are created. The cracks are created at random position rather than at certain specific positions.



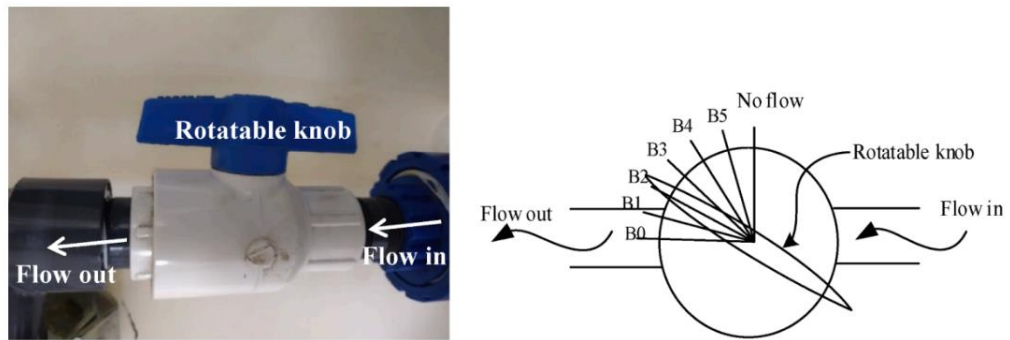
(Rapur & Tiwari, 2016)

Figure 5: Pump with Impeller Crack used in Rapur et. al (2016)

2.5 Blockage Modeling in the Experiment

Kumar et. al (2021) in their paper creates suction blockage by installing a mechanical modulating valve as shown in the Figure 6a. The valve is attached to the pipe upstream of the inlet of the pump and valve is configured such that five intermediate blockage conditions are created as shown in the Figure 6b. The valve can be adjusted

to any intermediate positions to simulate the blockage at the intake of the suction pipe inside the pump.



(Kumar, Dewangan, Tiwari, & Bordoloi, 2021)

Figure 6: (a) Mechanical Valve, (b) Blockage Positions

2.6 Softwares

2.6.1 ANSYS Meshing

Meshing is the process of creating two- or three-dimensional grids by dividing the complex geometries into elements of discrete domain. Meshing is one of the major workflows during the process of engineering simulation. Creating an optimal mesh serves as the cornerstone for engineering simulations and analyses.

ANSYS Meshing is one of the powerful and well-known software package tools used in CFD/FEA as ANSYS software suite for engineering simulation and analyses. It offers a comprehensive set of meshing capabilities, allowing users to generate high quality meshes of complex geometries. It is capable of generating high quality meshes for structural, CFD, electromagnetics, and explicit dynamics analysis. Fluid specific meshing, boundary layer refinement, multi-domain meshing is many of the key features of ANSYS Meshing for CFD cases. In the world of simulations and analysis using CFD, the ability to create high quality computational mesh of the physical domain is becoming increasingly essential and important. Some of the mesh generation tools available in ANSYS Meshing for CFD include:

- Automatic Meshing
- Patch Conforming Meshing
- Sizing Controls
- Inflation Layers
- Mesh Refinement
- Multizone Meshing
- Tetrahedra and Hexahedra Dominant Meshing

2.3.2 OpenFOAM

OpenFOAM is an open-source software designed for the CFD analysis. Chemical kinetics, turbulence, heat transport, and numerous other CFD issues are just a few of the many fields it may be used to simulate. Huang et al. (2019) in their paper has predicted the pump performances using both the OpenFOAM and ANSYS-Fluent. According to the paper, the OpenFOAM can be used to predict the pump performance with high degree of accuracy and the results obtained are comparable with the ANSYS results.

Xie (2010) studied the stator-rotor interaction using the OpenFOAM inside the ERCOFTAC Centrifugal Pump. The 2D and 3D models of the pump were generated to investigate the interaction between the flow in the impeller and in the diffuser. Both steady-state and transient simulations were employed for the study of the pump.

Smith (2016) investigates how well OpenFOAM can be used to simulate the stator-rotor interaction in the turbomachinery. The pump is simulated in full 3D transient mode using OpenFoam and compared with ANSYS CFX. The phenomenon of cavitation in pumps is also examined in the thesis. It is discovered that the outcomes predicted by the ANSYS CFX and the OpenFOAM are equivalent.

OpenFOAM can be used to simulate everything from laminar flows in the pipes to turbulent combustion of fuels. It has inbuilt capabilities for generating computational grids of a complex geometries, data processing and visualization tools.

Using OpenFOAM or any other CFD software requires a proper understanding of physics, numerical methods, as well as available computational resources (Maric, Hopken, & Mooney, 2021). Some of the solvers used for the CFD cases are as follows:

- simpleFoam: It solves the incompressible turbulent flows in a steady-state manner. The continuity and the momentum equation are solved by the solver using the SIMPLE technique.
- pimpleFoam: It is a transient solver that applies the PIMPLE algorithm to the pressure-velocity coupling in incompressible, turbulent fluid flows. Moving mesh and dynamic mesh are employed when the pimpleFoam solver is being used.
- icoFoam: It is a transient solver for fluids flowing laminarly and incompressibly.
- pisoFoam: It is a transient solver for turbulent, incompressible fluid flow. In order to couple pressure and velocity, it employs the PISO algorithm.

2.7 Steady-State Solver: SimpleFoam

For this research, simpleFOAM is selected as a solver to run the steady-state simulation of the centrifugal pump. It includes both the SIMPLE and SIMPLEC algorithm to use for pressure-velocity coupling. The Multiple Reference Frame (MRF) approach is used to perform the steady-state simulation. It is assumed that

there is no relative mesh motion between the stationary and spinning parts. For steady-state modeling, it is frequently referred to as the Frozen Rotor Method. In this case, the surrounding zones are solved using a stationary frame of reference, and the fluid zone inside the rotor region is modeled as a revolving frame of reference to produce the solution.

If a rotational frame of reference is chosen, a rotating object can be viewed as stationary through a transformation of the Navier-Stokes equation. The flow properties between the stationary and rotating regions are translated at the interfaces between them. The simpleFOAM does not take into consideration the transient effects of the flow. Thus, the solver provides fast results that can be used as an initial condition for the unsteady simulations.

Governing Equations

The simpleFoam employs the SIMPLE algorithm to solve the following basic governing equations:

1. Continuity Equation

$$\frac{\partial \rho}{\partial t} + \nabla \cdot (\rho \mathbf{U}) = 0 \quad (2.1)$$

Since, the simulation done is incompressible and steady. The temporal derivative term and the density can be removed from the simulation which results as follows:

$$\nabla \cdot \mathbf{U} = 0 \quad (2.2)$$

2. Momentum Equation

$$\frac{\partial(\rho \mathbf{U})}{\partial t} + \nabla \cdot (\rho \mathbf{U} \mathbf{U}) = -\frac{1}{\rho} \nabla P + \mu \nabla^2 \quad (2.3)$$

Removing the temporal derivative term and the density in the divergence term, the equation (2.3) then becomes:

$$\nabla \cdot (\mathbf{U} \mathbf{U}) = -\frac{1}{\rho} \nabla P + \mu \nabla^2 \mathbf{U} \quad (2.4)$$

where \mathbf{U} is the fluid velocity, P is the pressure and ρ is the density of the fluid.

2.8 Unsteady-State Solver: PimpleFoam

In order to perform the transient simulation of the centrifugal pump, pimpleFOAM is selected as a solver for turbulent incompressible flow. The pimpleFOAM is a

transient solver used for incompressible, turbulent flow of Newtonian fluids which uses the PIMPLE algorithm. The PIMPLE algorithm is a combination of the PISO and the SIMPLE algorithm. It can handle both the transient and steady-state simulations.

CHAPTER THREE: METHODOLOGY AND DESIGN STUDY

This chapter describes the methodology used for this research work, the research design, research methods and the tools used for the research.

3.1 Conceptual Framework

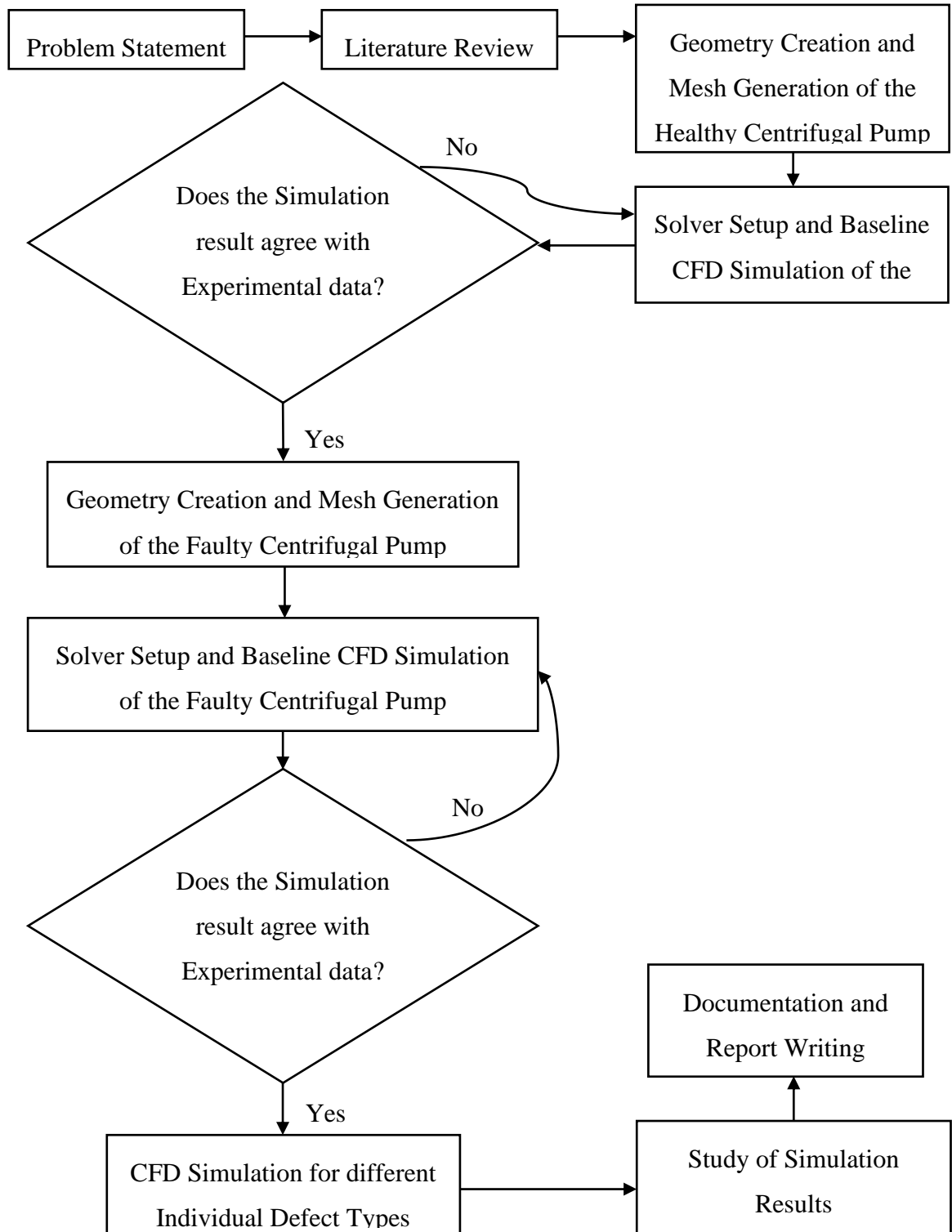


Figure 7: Flowchart for Research Methodology

3.2 Literature Review

This written paper is a thesis report for a research work on CFD simulation of a centrifugal pump. And for this, literature review for the CFD simulation of a centrifugal pump was conducted with the help of different articles, books and paper on centrifugal pumps, fluid flow. Various literature on the centrifugal pump and CFD simulation have been reviewed. This research thesis uses the centrifugal pump geometry same as that from Rapur & Tiwari (2019), Tiwari et al. (2020).

The research will be conducted as per the tasks listed below:

1. Geometry Modeling and Mesh Generation

The first and foremost task is to prepare a 3D CAD model of the centrifugal pump. The model CAD model of the pump, the fluid domain for centrifugal pump and the meshing of the computational domain is created during this time. Two models of the pump are modeled: First one is the model of the centrifugal pump without any fault and second one is the model of the pump with fault added on the geometry. After the geometry of the pump was created, the meshing of the computational fluid domain is created using ANSYS Meshing.

2. Solver Setup and Baseline Simulation

A turbulent incompressible fluid simulation will be performed in the OpenFOAM software for various cases.

3. Grid Independence Test

A grid independence test will be conducted to study the dependency of the solution obtained to the resolution of the mesh used in the computational domain.

4. Validation of the Simulation Results

For the validation of the simulation results, the results are first compared with the pump performance chart from the manufacturer and second with the experimental data provided by Kumar et. al (2021). Kumar et. al (2021) have collected two sets of time series pressure data using pressure transducer P-1 and P-2 in his paper to classify the blockage level.

Two pressure probes are set which records the fluctuation of static pressures as the simulation forwards in time. The probe location near the discharge pipe is termed

as Pressure Probe-1 and the probe location vertically above the eye of the impeller is termed as Pressure Probe-2 which can be seen as shown in the Figure 8.

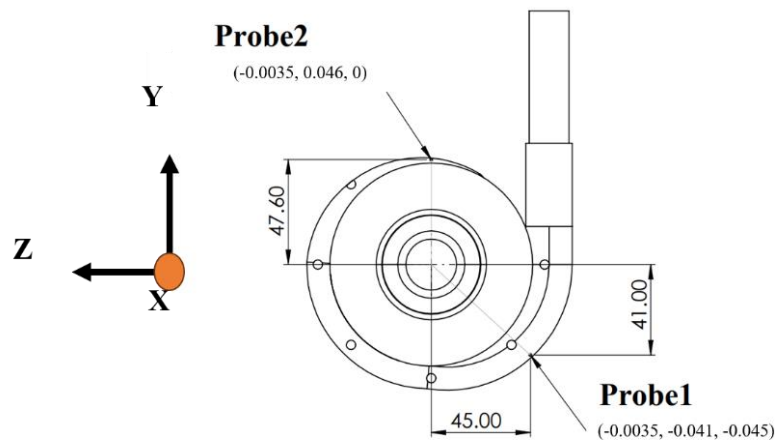


Figure 8: Coordinate Position of the Pressure Sensors used in Simulation

The pressure signals are collected for an extensive time period of 150 seconds with a sampling frequency of 5000. For the validation of the simulation results with the experimental data, the pressure signals are provided at pump running speed of 1800 rpm with no blockage condition.

5. Simulation Results Analysis

The results obtained from the simulation will be compared and validated with the pump performance chart and the experimental data available. The pump performance parameters such as flow velocity. Static pressure will be studied for a baseline and various fault cases.

6. Documentation and Report Writing

After the completion of the result analysis, the thesis report will be documented and will be submitted to the Department of the Mechanical and Aerospace Engineering, Pulchowk Campus.

3.3 Design Study

In this section, all the steps used while performing a CFD Simulation of a centrifugal pump will be described. An Oberdorfer 60P Series Centrifugal Pedestal Pump been chosen to perform the simulation.

3.3.1 Geometry Modeling and Mesh Creation

a) Centrifugal Pump without any Faults

The 3D model of the centrifugal pump without any fault was prepared initially as shown in the Figure 9. The CAD model of the pump was created using the SolidWorks software. The pump consists of following three components:

1. Inlet Cover Plate
2. Impeller Rotor
3. Volute Casing

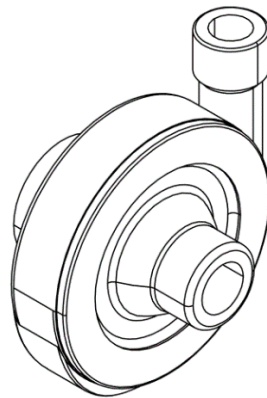


Figure 9: CAD Model of Oberdorfer 60P Pump

The Figure 10 below shows the exploded view of each component of the pump.

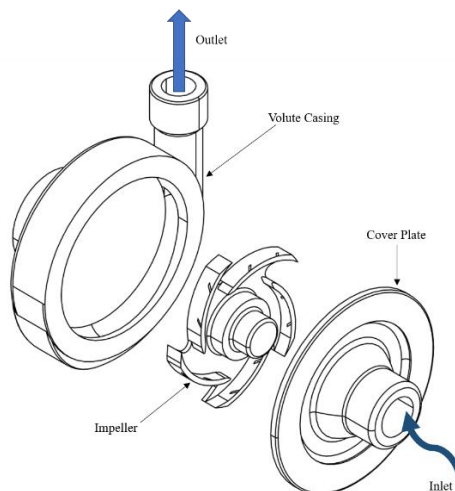


Figure 10: Exploded View of the Oberdorfer 60P Pump

The mesh was generated using the ANSYS Meshing. The fluid domain of the centrifugal pump is shown in the Figure 11.

1. Inlet Domain
2. Impeller Rotating Domain
3. Volute Domain

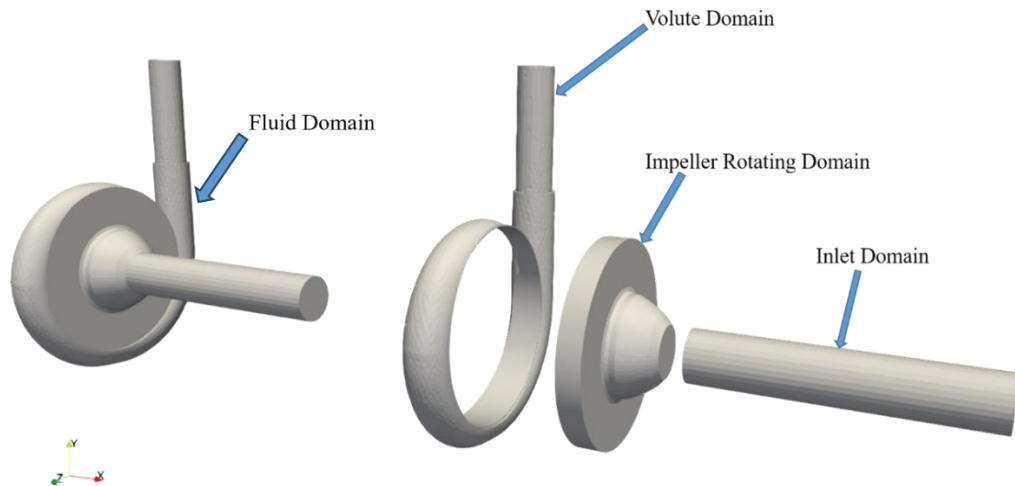


Figure 11: Computational Fluid Domain with Exploded View

After the preparation of the fluid domain, a mesh of appropriate size is created for the computational domain. The size of the mesh elements is selected such that the mesh independence is acquired. The total number of mesh elements used in the simulation is 336,087. The total number of the mesh elements that are used to generate the mesh of each sub domains are shown in the Table 2.

Table 2: Number of Elements for each domain

Domain	Element Number
Inlet	25160
Impeller	221880
Volute	89047

The mesh in the inlet domain is generated with structured grids whereas the impeller and the volute sub-domains are generated with unstructured grids. Inflation layer is added to capture the boundary layer near the wall of the inlet pipe. In the present

study, standard wall functions are used and thus, the y^+ values in a range of 30 – 500 satisfies the standard log-law (Versteeg & Malalasekera, 1995).

For the following flow conditions, the Reynolds number and estimated first cell height is calculated.

- $Y^+ = 30$
- Free Stream Velocity = 1.2105 m/s
- Reference Length = 23 mm
- Kinematic Viscosity = $1e-06 \text{ m}^2/\text{s}$
- Density = 1000 kg/m^3

The Reynolds number obtained is $2.8e+04$ and the estimated wall distance is $3.9e-04$ m. Obviously the flow is turbulent and thus the first cell height is set at 0.1 mm which is lower than the estimated wall distance 0.39 mm. The details of the inflation layer used in the inlet domain is given in the Appendix 4. This addition of inflation layer helps to understand the flow development inside the pipe by capturing the flow velocity near the wall accurately. An edge sizing with 40 number of divisions and a bias factor of 6 was applied along the length of the inlet pipe. i.e., the element size near the interface between impeller and inlet pipe is finer as compared to the start of the inlet pipe. The Figure 12 and 13 shows the image of the inlet domain with grids.

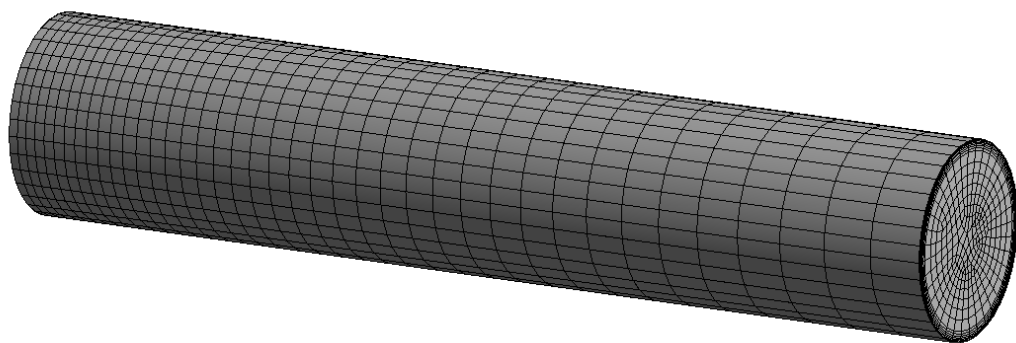


Figure 12: Structured Mesh used in the Inlet Domain

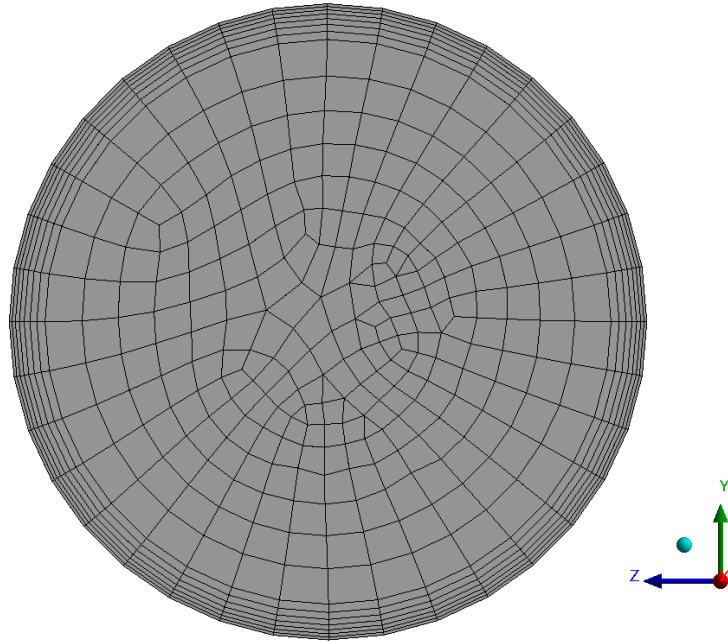


Figure 13: Mesh Showing Inflation Layer used in the Inlet Domain

The mesh used in the impeller rotor domain is of unstructured type with necessary refinement and face meshing applied. The mesh used in the impeller rotor domain is shown in the Figure 14.

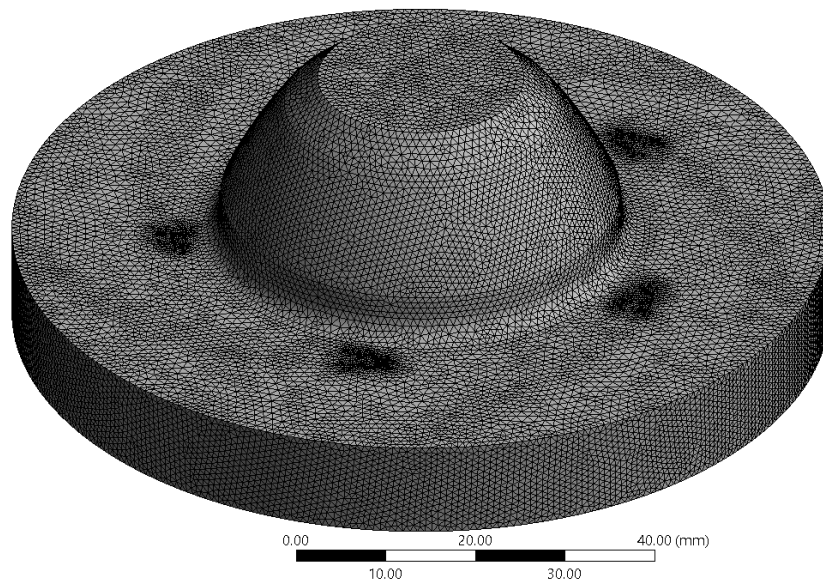


Figure 14: Mesh used in Impeller Rotor Domain

The mesh near the leading edge of the rotor blade is refined such that the geometry of the blade is well captured by the grids applied. The mesh applied in the surface of the impeller is shown in the Figure 15.

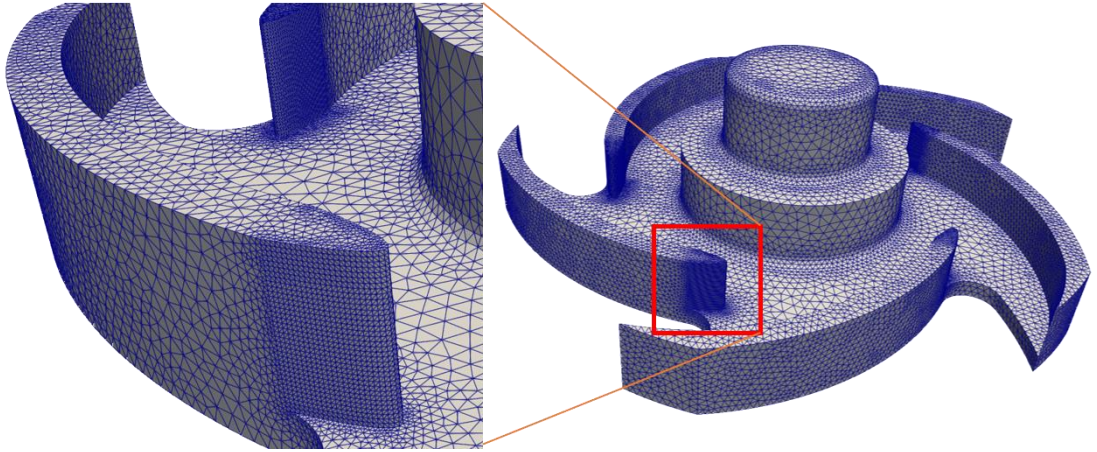


Figure 15: Surface Mesh used in the Impeller Blades

Similarly unstructured grids are used to create the mesh in the volute domain. The interface between the rotor and the volute is refined such that the number of mesh elements in both the domain are in equal amount. The mesh used in the volute domain is shown in the Figure 16.



Figure 16: Mesh used in the Volute Domain

b) Centrifugal Pump with Crack as a Fault

After the preparation of the geometry and the completion of meshing, the geometry was modified to incorporate the crack in the impeller as the fault. Also, the curved filleted region near shown as corners in the hub of the impeller is removed and a simple step is created for ease while meshing. To model the presence of crack in the top face of the impeller vane as used by Rapur et. al (2016) as presented in the *section 2.5*, five symmetrical rectangular cracks were added in the top face of each vane. The

depth of the crack was set as a parameter that can be varied to represent the severity of the crack. The impeller crack at the top face of the blade is shown in the Figure 17.

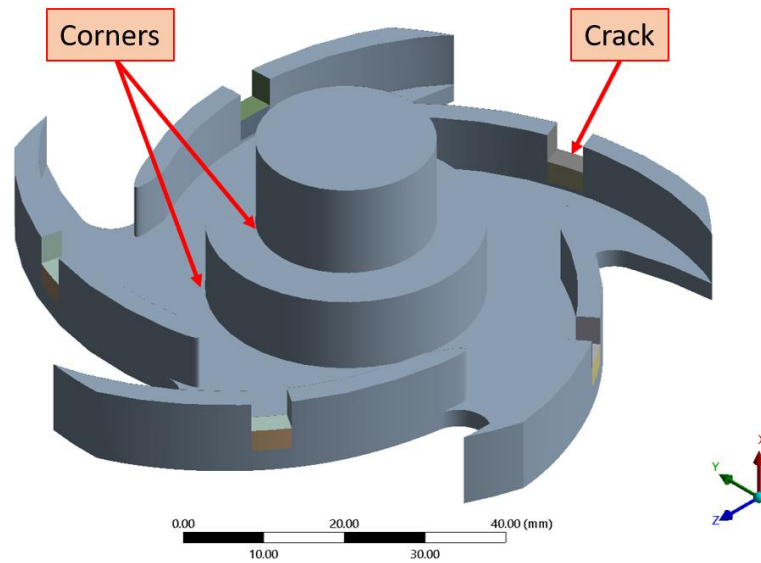


Figure 17: Impeller Crack

After the alteration in the geometry of the centrifugal pump to incorporate the crack, the meshing needs to be redone. Since, only the geometry of the impeller was altered, only the mesh of the rotating domain needs to be meshed again. The mesh of the inlet and the volute domain were unchanged. Near the crack zone, the grids were refined and face meshing was applied as well. The computational mesh which is used to discretize the crack in the blade is shown in the Figure 18.

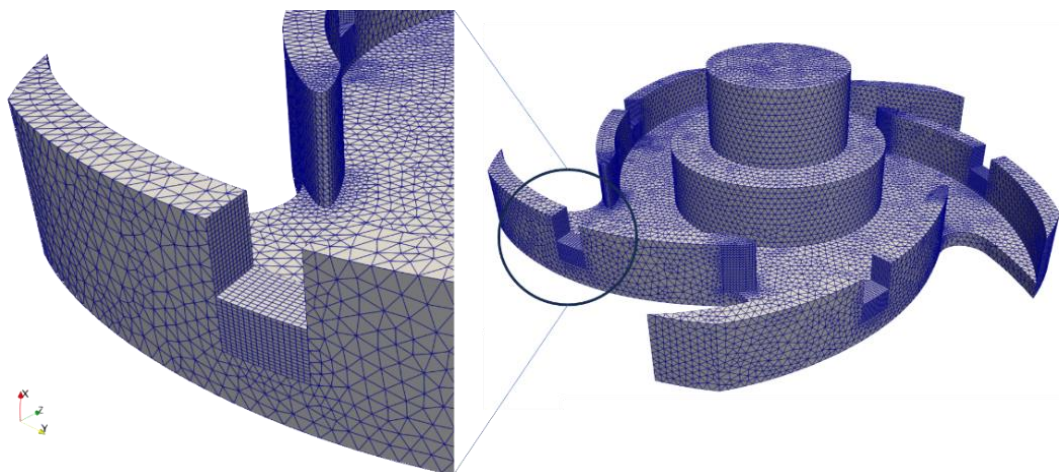


Figure 18: Mesh used in the Impeller with Faults

3.3.3 Solvers and Case Setup

After the creation of the mesh of the computational fluid domain, the mesh is imported into the openFOAM. The basic file structure of the openFOAM cases can be summarized from the Figure 19.

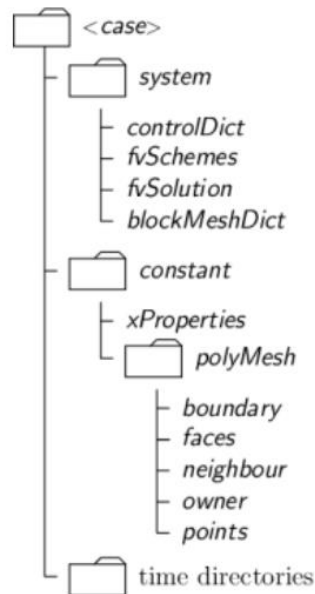


Figure 19: Basic OpenFOAM case Structure

Any openFoam case requires following three main directories: time directories, constant directory and the system directory. The time directory contains data files for individual fields such as p, U, k, omega, epsilon, nut, etc. The data inside the file can either be initial values and boundary conditions that the user must specify to define the CFD problem. The constant directory contains information of the physical and flow properties such as transportProperties, turbulenceProperteis, MRFProperties, dynamicMeshDict and others. Along with these properties, the constant directory contains a full description of the mesh used inside the polyMesh subdirectory. The system directory contains files associated with the solution procedure and the criteria for the mesh result convergence. It contains at least of three files mainly the controlDict, the fvSolution and the fvSchemes.

The following Table 3 provides the initial values and the boundary conditions applied inside the 0 subdirectory:

Table 3: Initial values and Boundary Conditions used in the Simulation

S.N.	Field Variables	Inlet Patch	Walls	Outlet Patch	Interfaces
1	U	flowrate InletVelocity	noSlip	inletOutlet	cyclicAMI
2	p	zeroGradient	zeroGradient	fixedValue	cyclicAMI
3	k	fixedValue	kqRWallFunction	inletOutlet	cyclicAMI
4	epsilon	fixedValue	epsilonWall Function	inletOutlet	cyclicAMI
5	omega	fixedValue	omegaWall Function	inletOutlet	cyclicAMI
6	nut	calculated	nutkRoughWall Function	calculated	cyclicAMI

In general, velocity inlet and pressure outlet are the most widely used boundary conditions for the simulation of a centrifugal pump. Other boundary conditions include pressure inlet-pressure outlet, total pressure inlet-mass flow rate outlet, etc. As for this simulation, velocity-inlet and pressure-outlet condition is set as a boundary condition. Steady-state CFD simulation of the centrifugal pump was done using simpleFoam using the Multiple Reference (MRF) approach. Here, the solver solves the governing equations for both the rotating and the stationary regions. The governing equations for the rotating regions contain an additional source term for Coriolis force. In the case of steady-state simulation, the head and the forces on the impeller blades are monitored for the convergence of the solution.

Similarly, transient CFD simulation of the centrifugal pump was done using pimpleFoam solver using the dynamic mesh approach. Here, the fluctuations of the head, the forces and the moments acting on the impeller blades are monitored with time for convergence. Also, two pressure probes at two different locations in the pump are set and the fluctuation of the static pressure at the two-probe location with time is also monitored and recorded. The code written for the MRFProperties and dynamicMeshDict is provided in the Appendix 2 and 3.

3.3.2 Grid Independence Test

Grid independence study refers to the state where the solutions of a simulation remain relatively unchanged as the mesh resolution is changed. It means that the outcome of the simulation is not explicitly affected by the size of the grid. For the mesh independence study, the element size is increased in successive steps and the accuracy of its corresponding solution is examined. Generally, refined grid consists of larger element size which in turn increases the computational time. Whereas, coarsened grid results in a smaller number of element size thereby decreasing the computational time. Therefore, it is critical to perform grid independence study in order to ensure a balance between solution accuracy and computational time efficiency.

To select a proper computational grid for the simulation, a grid independence test was carried out. The pump was run at 1800 rpm and a mass flow rate of 0.504 LPS was supplied as an inlet boundary condition. A kinematic pressure of 101.325 was applied at the outlet patch as a pressure-outlet boundary condition. Steady state simulation was ran using the simpleFOAM. The number of the grid size was increased gradually from 60K element to 400K elements in order to check the independence the result from the resolution of the grid used in the simulation. The Figure 20 below shows the result obtained from the grid independence test in openFOAM with the standard k- ϵ turbulence model.

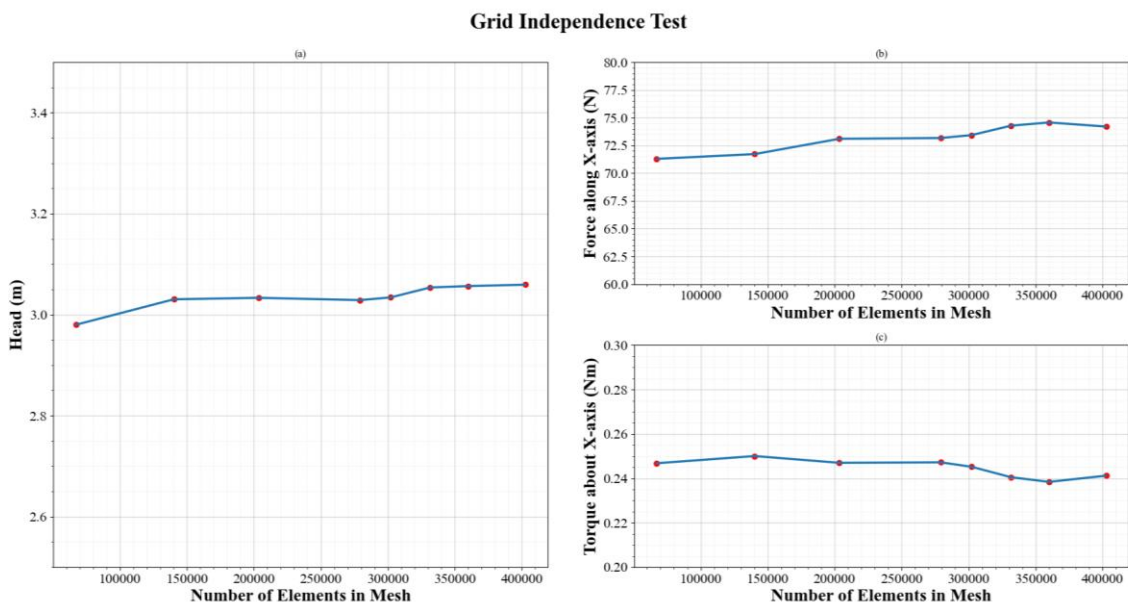


Figure 20: Grid Independence Test

The Figure 20a shows the plot of the head calculated as the number of the mesh resolution is increased. The x-axis shows the number of the mesh element and the y-axis shows the value of the head calculated respectively. The Figure 20b shows the plot of force acting on the surfaces of the rotor along the x- direction as the mesh resolution is increased. Similarly, the Figure 20c shows the plot of torque generated by the rotor about the x-axis

At coarser mesh at around 70K number of mesh element, the head calculated was about 2.98 meters. As the number of the mesh element was increased, the value of the head calculated was converged at around 3.05 meters. When the number of the mesh element was increased above 350000, the effect of the grid changes on the calculated head was negligible. The head difference between the following two mesh of sizes 331679 and 360053 was only 0.3%. Thus, the mesh with lower mesh count was selected and this completes the grid independency test for the fluid domain. So, with a computational grid of around 300000 – 350000 mesh elements the test yields acceptable results. The table used while generating the Figure 20 is provided in the Appendix 5.

CHAPTER FOUR: RESULTS AND DISCUSSION

In this chapter, the results from the CFD simulation are presented and discussed.

5.1 Simulation Results Validation

A series of simulation are done in order to validate the approach used in our simulation. At first the results obtained are compared with the performance chart from the manufacturer of the Centrifugal pump: Oberdorfer 60P. After the validation from the performance chart, static pressure values at two probe location as a pump performance parameter is compared with the data provided by Kumar et. al (2021) with paper titled “Identification of inlet pipe blockage level in centrifugal pump over a range of speeds by deep learning algorithm using multi-source data”.

5.1.1 Result Validation with Pump Performance Chart

The pump performance chart for the Centrifugal Pump Oberdorfer 60P is shown in the Appendix 1.

- **At Inlet Discharge of 0.5LPS**

A number of steady-state simulations are performed at a fixed inlet discharge of 0.5 LPS by varying the rpm of the impeller from 1725 rpm to 4000 rpm. The head obtained from the openFOAM at 0.5LPS with varying rpm are compared with the head from the performance chart. The Figure 21 shows the graph of head versus the rpm at the inlet discharge of 0.5LPS:

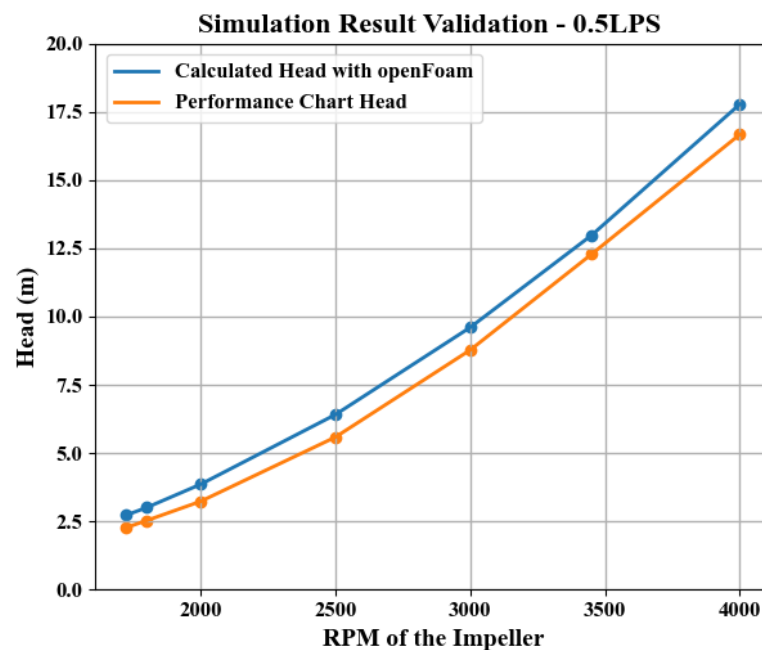


Figure 21: Result validation at 0.5LPS

The Figure shows a close agreement between the results from the simulation and from the performance chart. The head predicted by the openFOAM are higher than the head given by the pump performance chart with a mean head difference of 0.715 meters

- **At Rotor Speed of 3000 RPM**

A series of steady-state simulations are run at a fixed rpm of 3000 by varying the inlet discharge from 0.12 LPS to 0.75 LPS. The head predicted by the openFOAM is then compared with the head from the performance chart. The head given by the openFOAM at low inflow rate agrees with the head from the performance chart. But at higher discharge rate greater than 0.5 LPS, the head predicted by the openFOAM does not agree with the performance chart as shown in the Figure 22. Since, at high rpm with high discharge rate, the turbulence inside the pump gets increased. Thus, the use of the turbulence model kEpsilon on the simulation might have some effect on the results of the head obtained from the openFOAM.

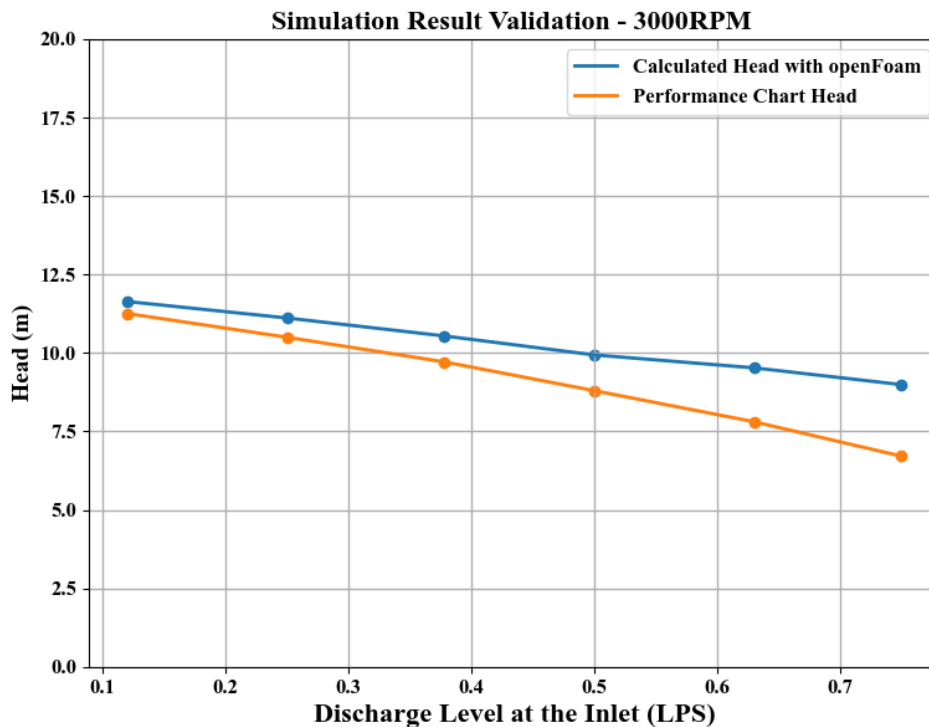


Figure 22: Result validation at 3000 RPM

- **At Rotor Speed of 1725 RPM**

Steady state simulations are performed for a base rpm of 1725 by varying the inlet discharge value. The Figure 23 shows a graph of head versus discharge.

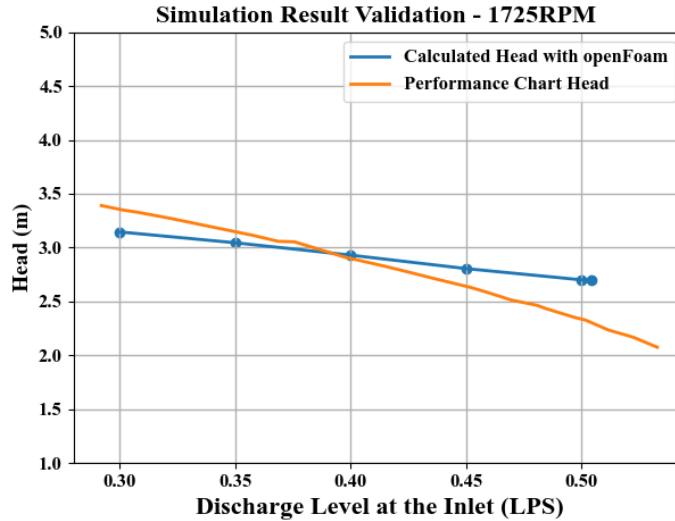


Figure 23: Result validation at 3000 RPM

The discharged at the inlet is varied from 0.3 to 0.504 LPS. The result shows a close agreement between the simulation and performance. From 0.3 to 0.504 LPS, the head obtained are close enough, but after this range of flow rate, the head calculated from the OpenFOAM differs with the head from the chart.

5.1.2 Result Comparison with the Experimental Data

- **Pump Performance at 1800 RPM**

Kumar et. al (2021) performed some preliminary performance test of the pump at 1800 rpm. For the validation with the experiment, a series of steady-state simulation was performed in openFOAM at 1800 rpm for various flow rate.

The Figure 24 shows a plot of head versus flowrate for both the simulation and the experiment.

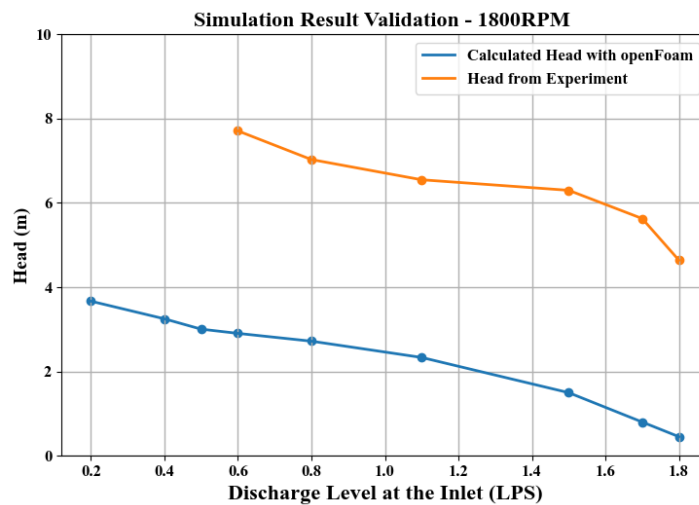


Figure 24: Experimental Validation of the Simulation

The plot shows distinctly that the results from the simulation does not agree with the experimental data. The experimental data are way above the simulation results as well as performance data provided by the manufacturer. The data from the pump performance chart and the simulation results from the OpenFOAM agrees with each other but for the case of the experimental data, the data at 1800 rpm does not match and might be some errors while doing measurement.

- **FFT analysis of the Pressure Signals**

The FFT analysis of the pressure signals provided by Kumar et. all (2021) is done for a 10 second period. The data available is for pump running with a speed at 1800 rpm. The FFT analysis of the signal shows that the major components that comprises the pressure signal are at frequencies of 307 Hz, 262 Hz, 140 Hz respectively as shown in the Figure 25 and 26.

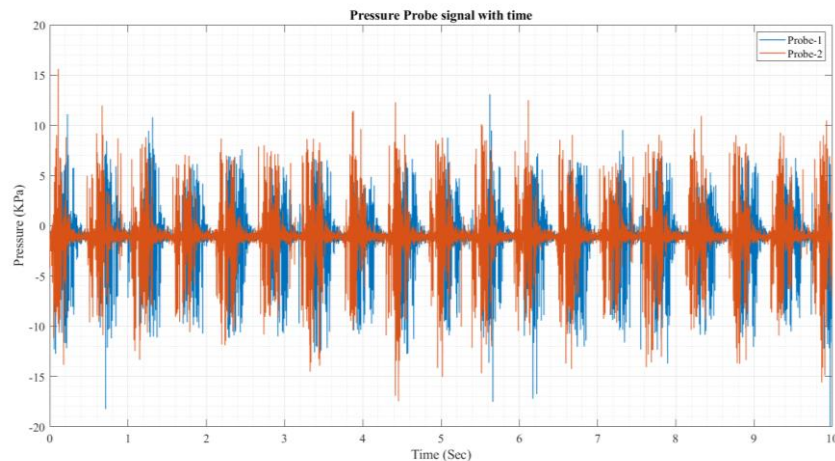


Figure 25: Pressure Signal with Time - Experimental

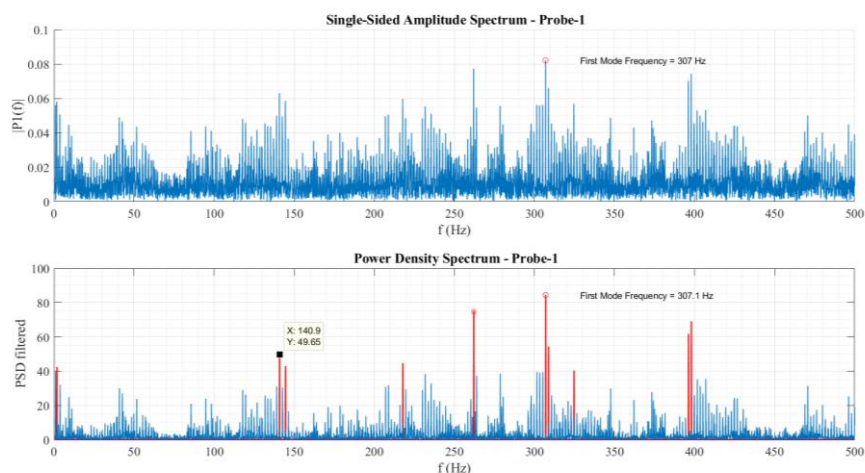


Figure 26: FFT of the Pressure Signal at Probe-1 – Experimental

- **Simulation Result at Rotor Speed of 1800 RPM**

A transient simulation is run at rpm of 1800 with inlet discharge of 0.5 LPS. The pressure signals are recorded at a time step of 5×10^{-5} sec. At this 1800 rpm, the impeller takes about 0.03333 sec to complete 1 cycle which is about 30 Hz in frequency. Thus, the impeller blades cross the pressure probe at about 0.0066 sec which is about 150 Hz for each rotation. So, the pressure signal must have a frequency content at this range and must be the major contributor of the pressure signals in overall.

The FFT of the signal at the pressure probe-1 shows a frequency peak at about 155.8 Hz whereas the FFT of the signal at the pressure probe-2 shows a frequency peak at about 150 Hz which seems to be in certain agreeable range. Also, from the PSD diagram, it is seen that the power content of the pressure signal is also in this frequency value. The pressure signals with time and the FFT of both pressure signals are provided in the Figure 27, 28 and 29.

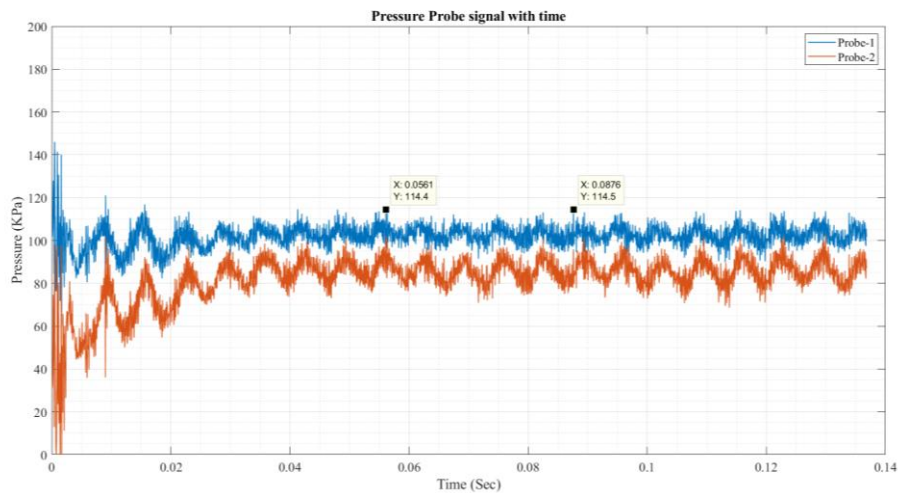


Figure 27: Pressure Signal with Time – 1800 RPM

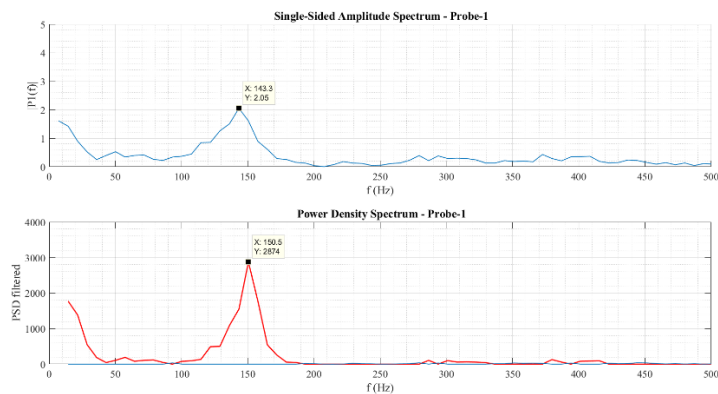


Figure 28: FFT of the Pressure signal at Probe 1 – 1800 RPM

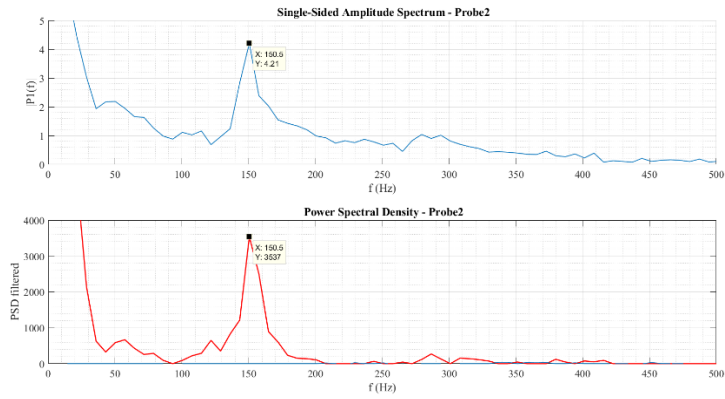


Figure 29: FFT of the Pressure signal at Probe 2 – 1800 RPM

- **Simulation Results at Rotor Speed of 3000 RPM**

A transient simulation is run at a rpm of 3000 with a base inlet discharge of 0.5 LPS. The pressure signals are recorded at a time step of 8×10^{-6} . At this 3000 rpm, the impeller takes about 0.02 sec to complete 1 cycle which is about 50 Hz in frequency. Thus, each impeller blade has to pass the pressure probe exactly at about 0.004 sec which is about 250 Hz. So, the pressure signal at 3000RPM must have a frequency content at 250 Hz and must be the major contributor of the pressure signals in overall.

The FFT analysis of the pressure signal shows that the frequency in this range is the major contributor. The FFT of the signal at both pressure probe-1 and pressure probe-2 shows a frequency of about 254.51 Hz. Also, from the PSD diagram, it is seen that the pressure signals from this frequency value comprises majority of the power spectrum. The pressure signals with time and the FFT of both pressure signals are provided in the Figure 30, 31 and 32.

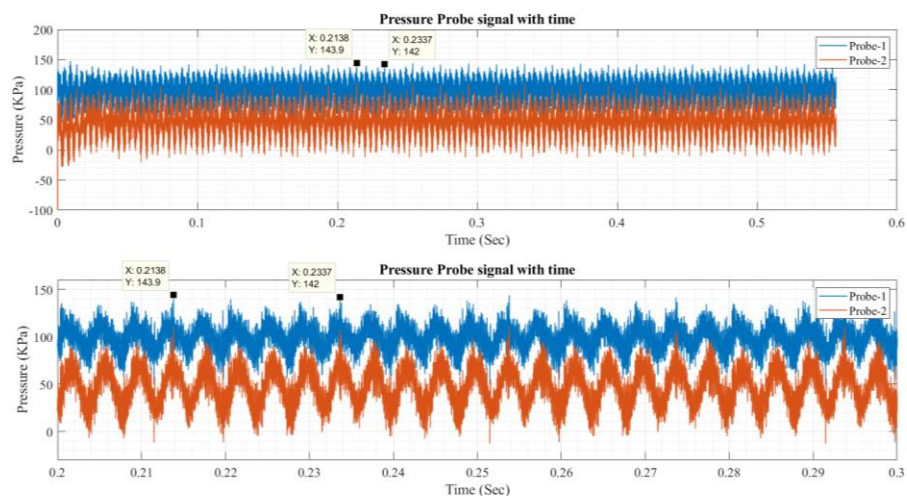


Figure 30: Pressure Signal with Time – 3000 RPM

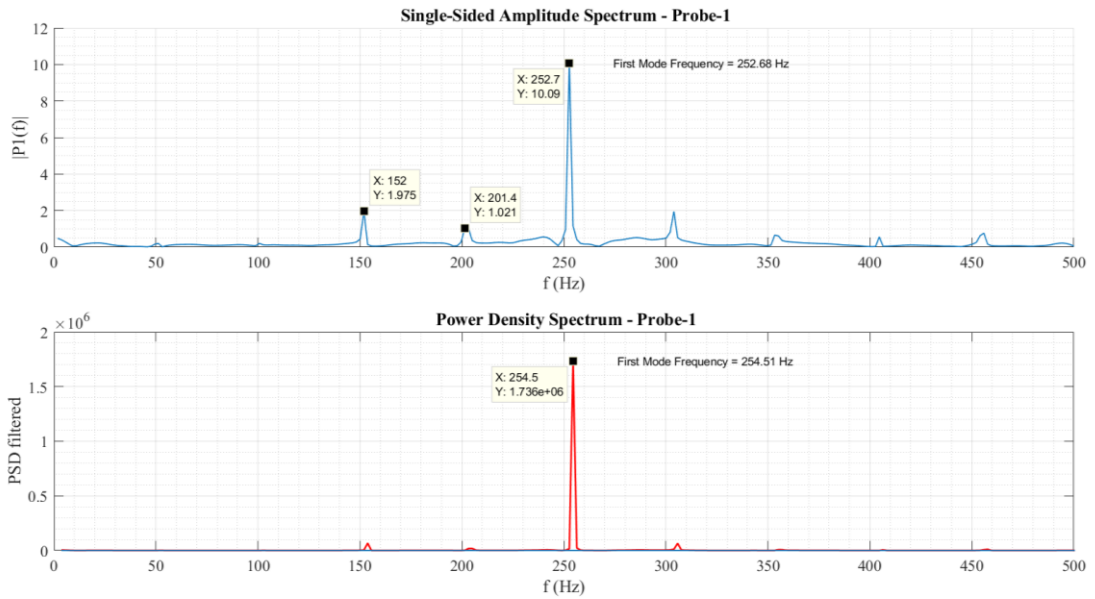


Figure 31: FFT of the Pressure signal at Probe 1 – 3000 RPM

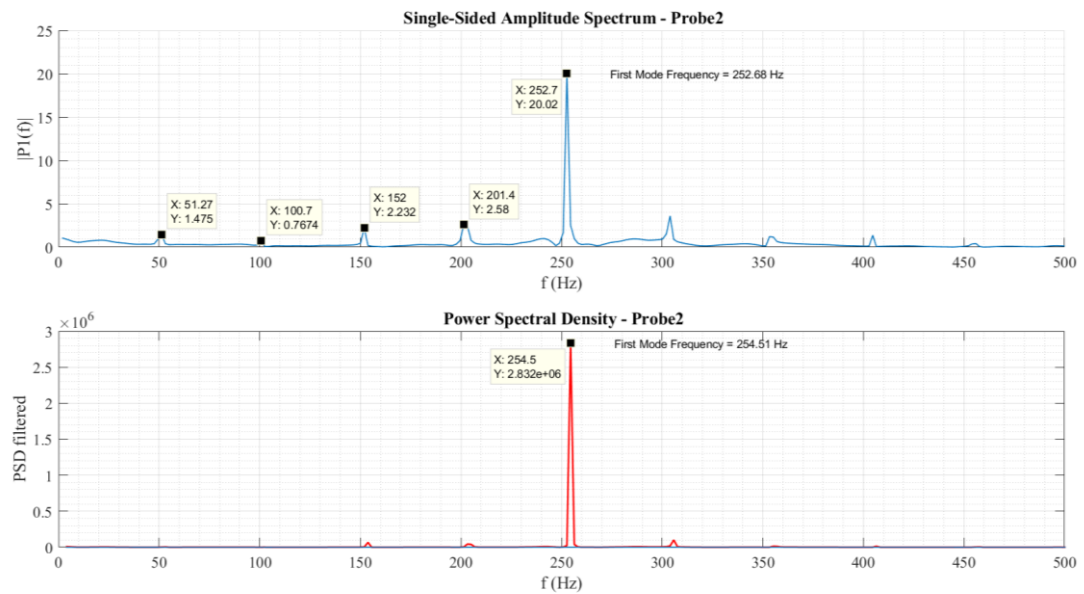


Figure 32: FFT of the Pressure signal at Probe 2 – 3000 RPM

The results from the simulation quite doesn't agree with the results from the experimental data. In case of the transient simulation at 1800 RPM, the major contributor the pressure signal is at around 150 Hz. But from the experimental data, it shows that the major contributor is at 307 Hz. Also, the experiment data has a peak at about 140.9 Hz which might corresponds to our 150 Hz frequency peak.

In case of 3000 rpm, a frequency peak of 250 Hz was expected and a frequency of 254.51 Hz was found from our simulation results.

5.2 Simulation Results on the Blockage

Both the Steady state and Unsteady state CFD simulation of the centrifugal pump is run with various inlet conditions i.e., by varying mass flow rate at the inlet and respective flow behavior is monitored. The variations of the mass flow rate at the inlet corresponds to the severity of blockage at the inlet. To study the fluctuations of variables in the flow field due to blockage, pressure and velocity contours are plotted for various mass flow rate at the inlet. Also, two pressure probes are placed in the fluid domain to study the pressure fluctuation with time for transient simulation.

5.2.1 Pump Flow Development

The results of the flow fields obtained from the simulation is visualized using ParaView software which is one of the utilities used for postprocessing the results obtained from the openFOAM. The simulation is run at a base rpm of 3000 at the inlet flow rate of 0.63 LPS. The Figure 33 shows the development of flow field velocity vectors inside the centrifugal pump by steady-state simulations. From the figure below, it can be seen that the flow velocity increases till the fluid reaches the impeller outlet as shown by the red arrow vectors. Then, the flow velocity starts decreasing with the opening of the volute passage.

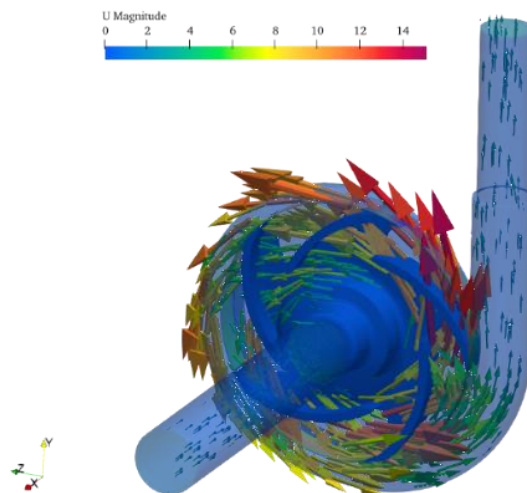


Figure 33: Flow Develop inside the Pump (steady-state)

The Figure 34 shows the flow development inside the inlet pipe. Here, the boundary layer grows from right to the left of the inlet pipe. The flow velocity increases near the small section which connect the inlet pipe and the impeller head region. This may be due to the reason that the fluid comes in contact with the impeller onwards and the

rotation of the impeller imparts the motion to the fluid. Also, the flow velocity is larger near the outlet of the impeller.

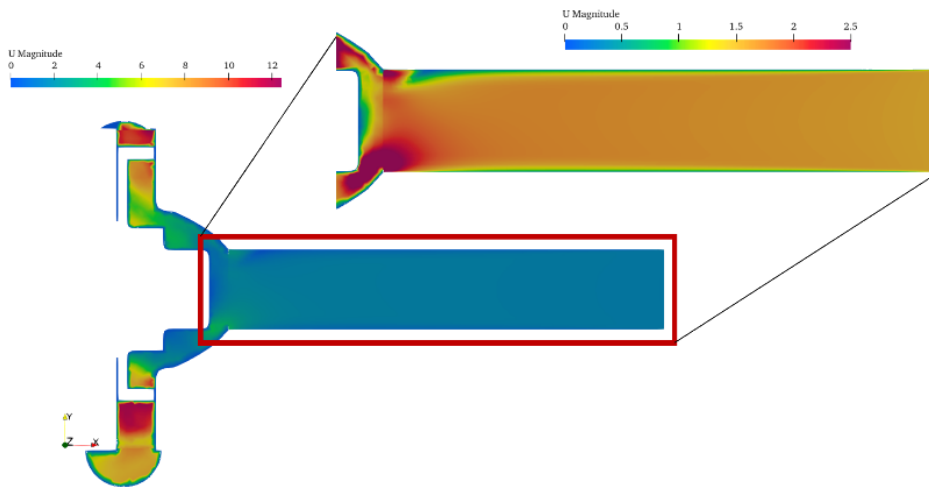


Figure 34: Developed Flow at Inlet Section

Figure 35 shows the flow development at the outlet section of the centrifugal pump showing the impeller with the blades. The velocity flow field increases from the eye of the impeller till the outlet of the impeller. The velocity then starts to drop down with the opening of the volute passage. The velocity decreases till the flow reaches the Region A. After this, the flow develops and the velocity becomes constant as shown in zoomed section of the outlet pipe. The flow velocity once again increases after it encounters a step in the outlet pipe.

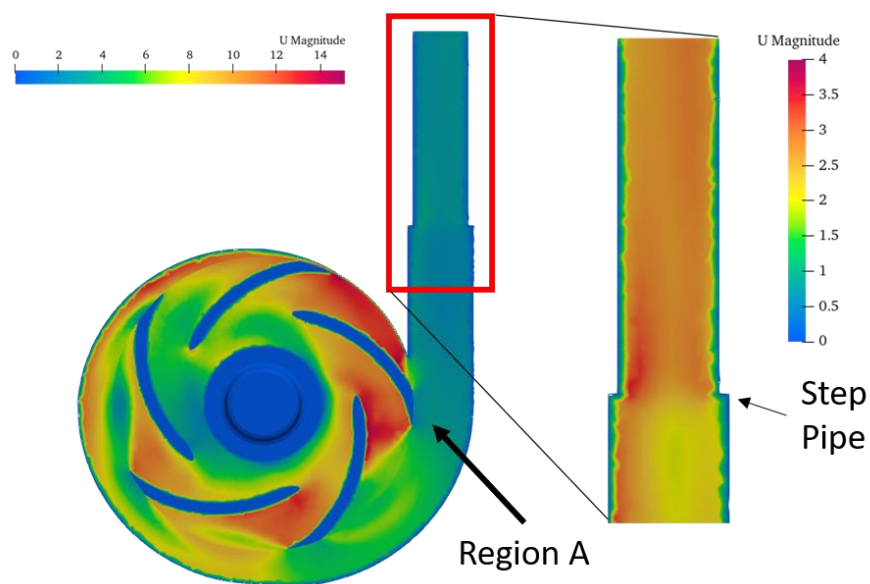


Figure 35: Flow at Outlet Pipe

5.2.2 Pressure Distribution

The decrease in the inlet flow rate leads to the decrement in the local static pressure at the inlet section of the pump. The change in static pressure across the pump domain increases with severity of the blockage level. The minimum static pressure decreases and the maximum static pressure increases.

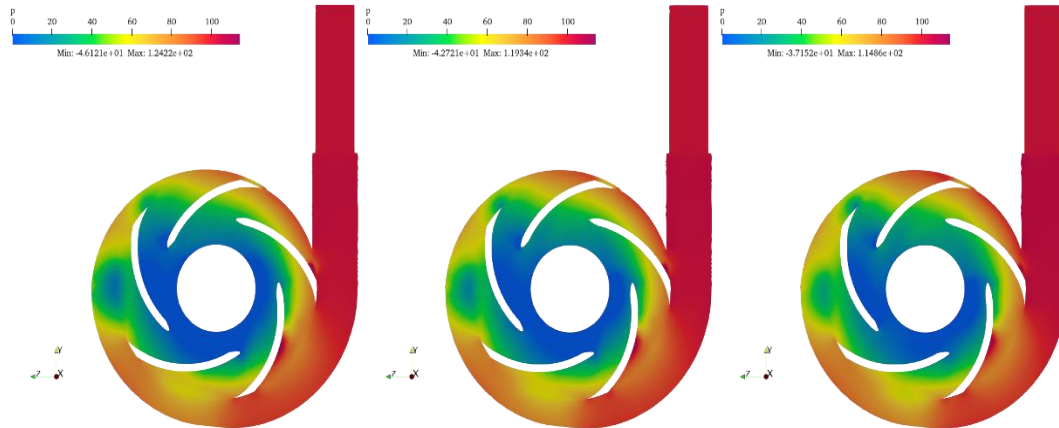


Figure 36: Static Pressure Distribution in the pump (steady-state) left: 0.504 LPS, mid: 0.63 LPS, right: 0.757 LPS

Since with the introduction of blockage, the flow rate decreases which in turn decreases the flow velocity inside the pump. With successive decrease in the inlet flow rate from 0.757 LPS to 0.504 LPS, the minimum static pressure is in decreasing trend from -37.152 to -46.12 as shown in the Figure 36. However, the maximum static pressure is in the increasing trend from 114.86 to 124.22. Thus, the change in the static pressure i.e., the difference between the minimum and the maximum static pressure increases with the introduction of the blockages. In overall, with the blockage present, the average flow velocity gets decreased which increases the change in static pressure across the fluid domain.

5.2.3 Flow Field Velocity Vectors

The Figure 37 shows the flow velocity vectors plotted for three discharge cases. With decrease in inlet flow rate, the maximum flow velocity inside the pump gets reduced from 15.766 to 15.26.

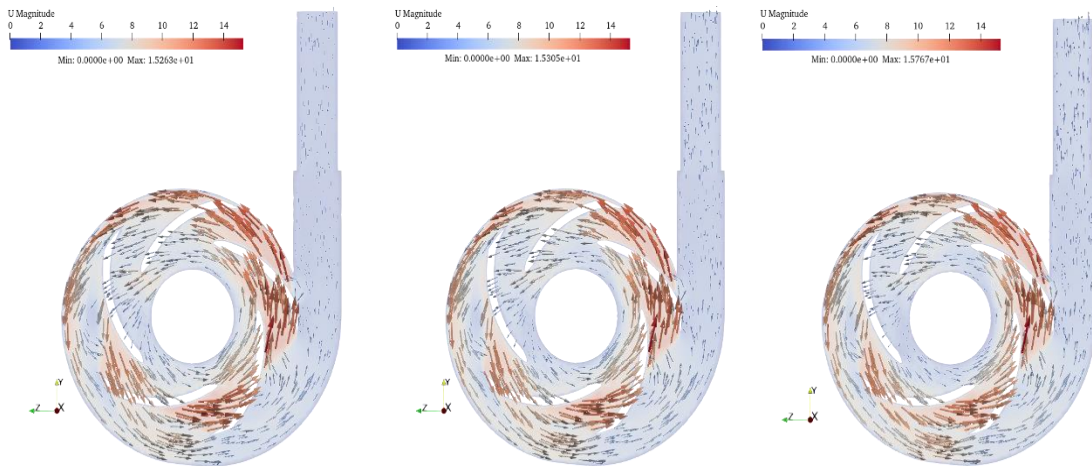


Figure 37: Velocity Vectors in the pump (steady-state) left: 0.504 LPS, mid: 0.63 LPS, right: 0.757 LPS

5.2.4 Static Pressure and Flow Velocity with Blockage

With the occurrence of blockage upstream of the inlet pipe, the total amount of fluid that enters the inlet decreases which results in the reduction of the mass flow rate at the inlet of the pipe. With this reduction of the mass flow at the inlet, the flow velocity decreases along the pump domain, the static pressure at the inlet section of the pump decreases which is one of the main reasons for the occurrence of the cavitation inside the pump in the future. A study on the variation of the pump performance parameters such as flow velocity and static pressure is done by performing a series of steady-state simulation at a base rpm of 1725. The Table 4 shows the value of the static pressure at the probe position 1 and 2 along with the flow velocity at the inlet and outlet of the pump.

Table 4: Study of pump performance with Blockage level

S.N.	Blockage (LPS)	P1	P2	P_inlet	P_outlet	Mag-(U _x) at inlet	Mag-(U _y) at outlet
1	0.5	-0.5310	-5.0715	-25.511	0	1.20957	1.99691
2	0.496	-0.5968	-5.1489	-25.588	0	1.19989	1.98036
3	0.49	-0.6442	-5.2667	-25.711	0	1.18538	1.95637
4	0.48	-0.7349	-5.4896	-25.889	0	1.16118	1.91584
5	0.47	-0.7627	-5.6355	-26.070	0	1.13699	1.87586
6	0.46	-0.8467	-5.8541	-26.28	0	1.16111	1.83599
7	0.455	-0.8758	-5.9506	-26.373	0	1.11280	1.81672
8	0.45	-0.9050	-6.0431	-26.467	0	1.08861	1.79709

Since, with presence of blockage, the inlet discharge gets reduced. Increasing the blockage level means decreasing the volume flow rate at the intake of suction pipe. In the Table 4, the 0.5 LPS shows a base discharge and all other lower discharge values represents the presence of blockage level in the pipe. Static Pressure in openFOAM is shown as kinematic pressure. During this simulation, the static pressure of 0-gauge pressure is applied at the outlet of the pump. Thus, all the static pressure values shown above are negative.

The blockage level at the inlet of the pipe is increased by decreasing the inlet flow rate at a base rpm of 1725. The static pressure at the inlet keeps on decreasing from -25.52 to -26.47. So, the net effect would be to increase the change in static pressure across the whole pump domain. The Figure 38 shows a plot of the variation of the static pressure with increasing amount of blockage level at the two-probe position and also at the inlet of the pump. Whereas the Figure 39 shows the variation of the magnitude of the Y-Velocity at the outlet of the pump.

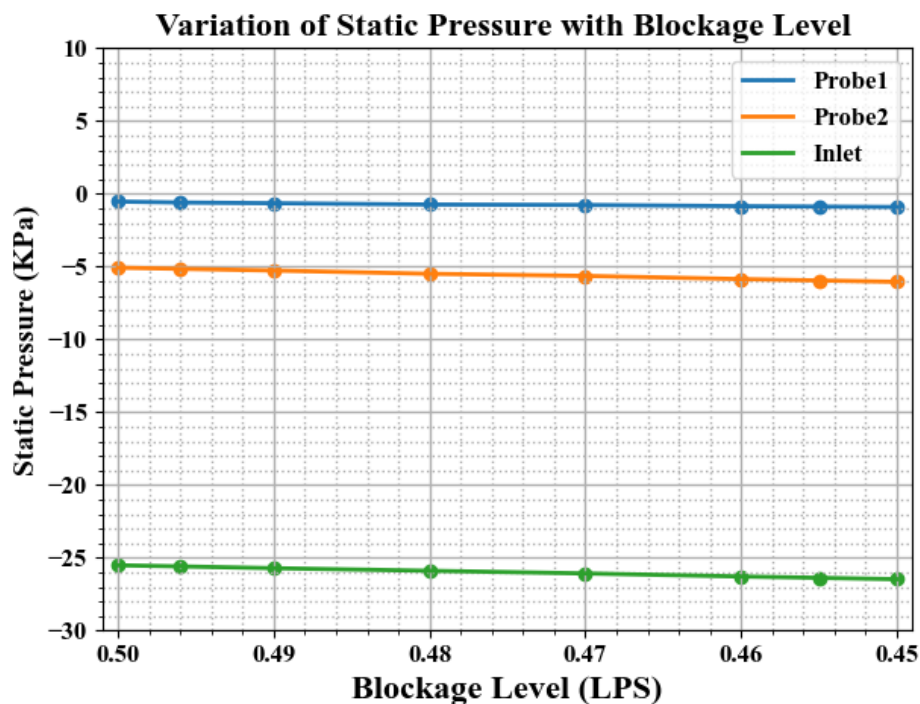


Figure 38: Static Pressure Variation with Blockage

From the plot shown in the Figure 38, it is evident that the value of the static pressure at all these three positions i.e., at the two-probe position, probe1 and probe2 and at the inlet patch of the pump decreases with the increase in the blockage level.

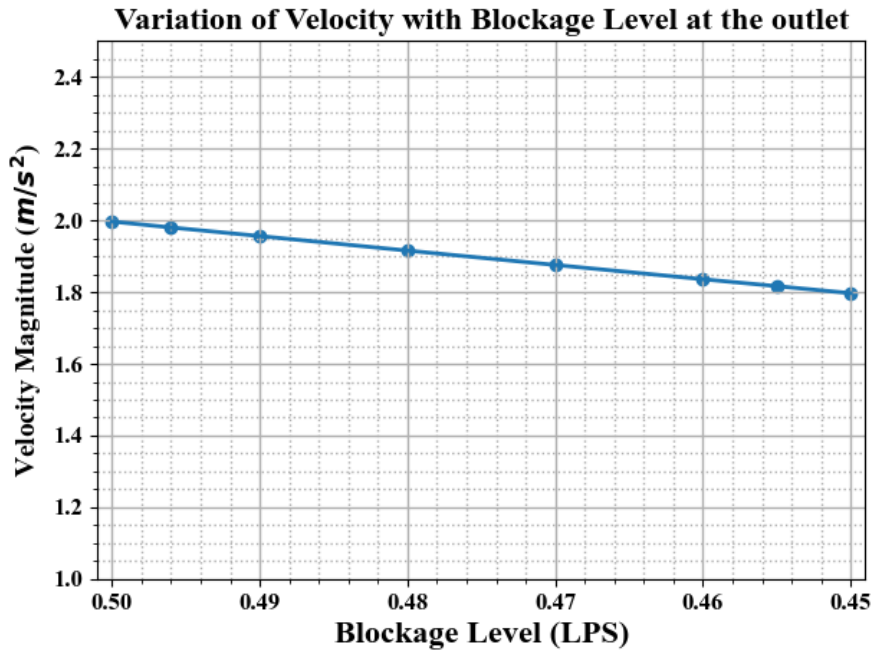


Figure 39: Mag (U_y) Variation with Blockage

Also, from the plot in the Figure 39, it is seen that the magnitude of the y – velocity at the outlet of the pump decreases with the introduction of the blockage. For a base inlet flow rate of 0.5 LPS, the magnitude of the y – velocity is around 2 m/s whereas with the decrease in the inlet flow rate, this magnitude of y – velocity keeps on decreasing.

So, the proper monitoring of the pump flow parameters such as the static pressure and the velocity magnitude at various position across the pump helps in ensuring the occurrence of faults such as blockage.

5.3 Simulation Results on the Impeller Crack

A rectangular crack was added as a fault on the top face of every blade of the impeller as shown in the Figure 40.

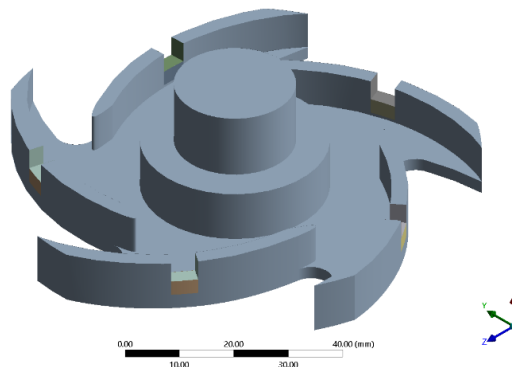


Figure 40: Impeller Fault with crack at the top on the blades

The length and width of the crack was fixed while the depth was varied from 3.8 mm to 4.4mm in a step of 0.2mm. The steady state simulations were performed for four cases of crack with depth varied from 3.8mm to 4.4mm while the transient simulations were performed for three cases of crack depth from 4.0mm to 4.4mm. The static pressure at the two probe locations is collected in both the simulation. The static pressure values from the steady-state simulation are provided in the Table 5:

Table 5: Variation of Static Pressure with Crack Depth

S.N.	Crack Depth (mm)	Probe1 (kPa)	Probe2 (kPa)
1	3.8	102.32	93.7
2	4	102.153	92.87
3	4.2	102.03	91.332
4	4.4	101.988	91.261

The values of the static pressure keep on decreasing at both the probe locations when the crack depth is increasing. Thus, severe occurrence of crack significantly decreases the static pressure all over the pump domain thus leading to the occurrence of cavitation at regions where the local static pressure goes below the local static vapor pressure. The static pressure values from the transient simulations were used to perform the FFT analysis on the pressure signal from the probe 1 with the sampling rate of 2×10^{-4} seconds. The simulation was done at 1800 RPM for approximately 3 revolutions of the impeller. The following sections describe the results obtained from the FFT analysis:

- **Crack Depth of 4mm**

The static pressure recorded in the two probe locations is plotted with time and is shown in the Figure 41:

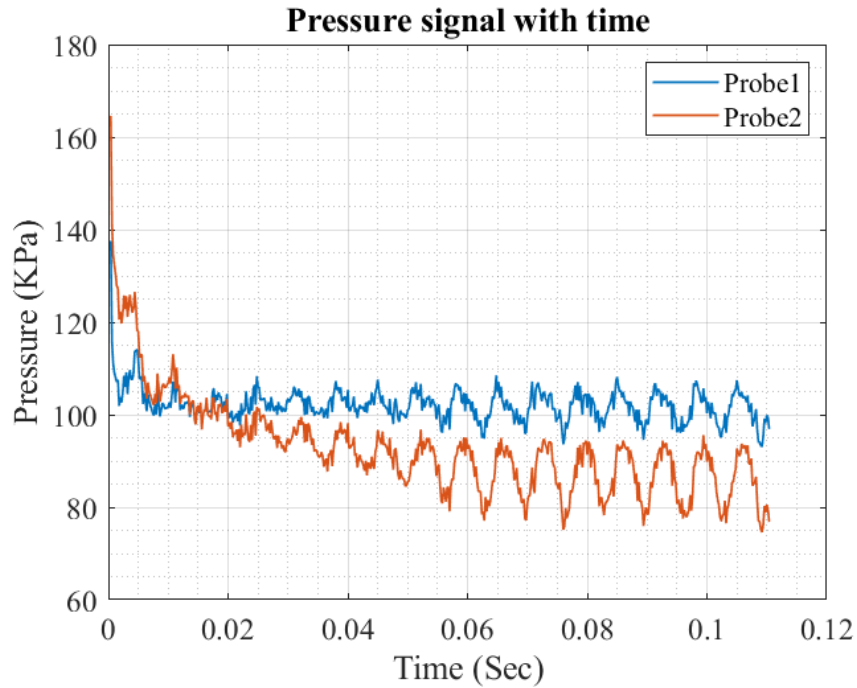


Figure 41: Static Pressure values with time

The time taken by the impeller to rotate a complete revolution is 0.033 seconds which is about 30.30 Hertz. Also, the time for one of the single blades to cross the probe location is 0.0066 seconds which is about 151.51 Hz. The FFT of the signal shows a frequency spike at 27.22 Hz, 145.19 Hz and 300 Hz. These obtained frequencies can be associated with the 1st, 5th and 10th harmonics for a fundamental frequency of 30.3 Hz.

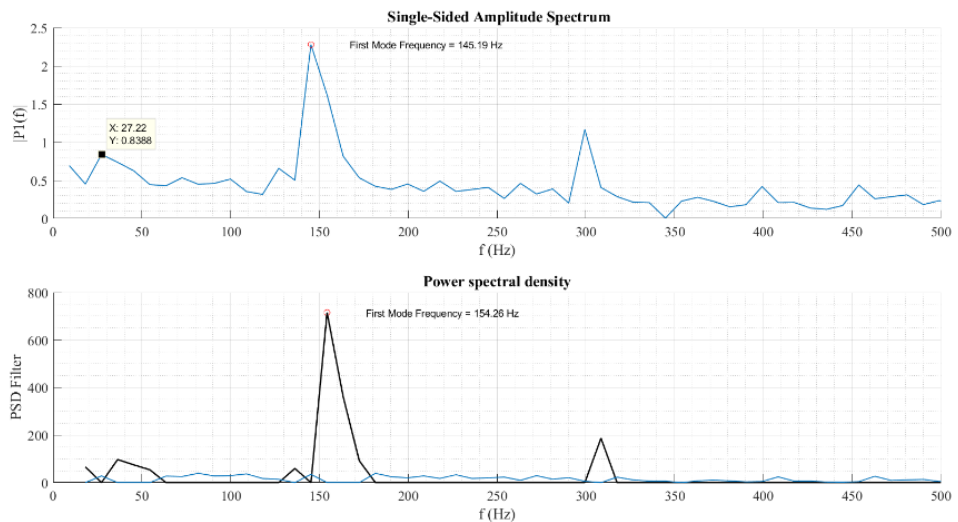


Figure 42: FFT-4mm crack

- **Crack Depth of 4.2mm**

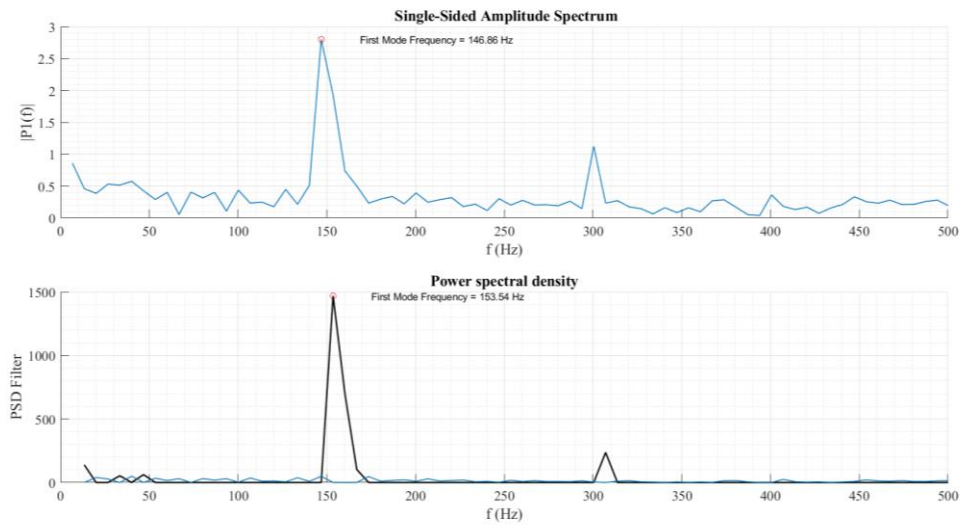


Figure 43: FFT-4.2mm crack

- **Crack Depth of 4.4mm**

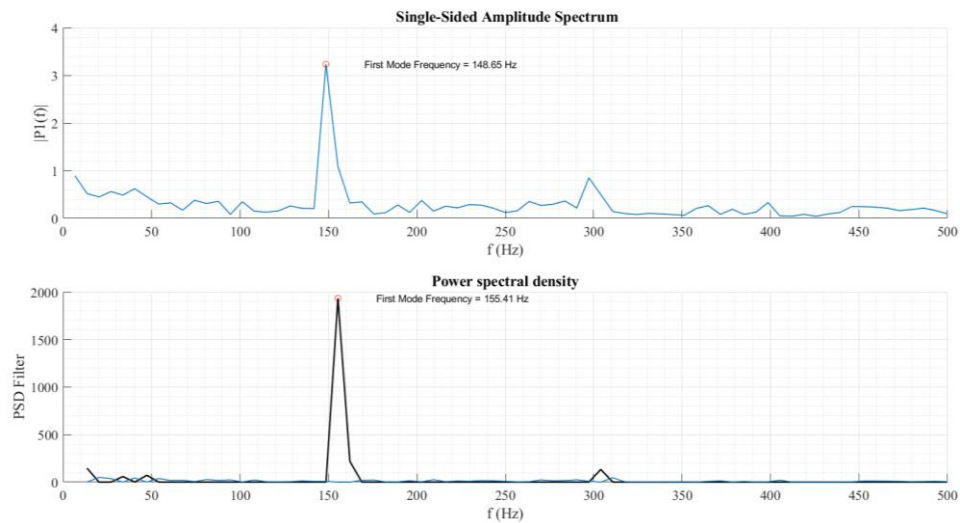


Figure 44: FFT-4.4mm crack

The top subplot as shown in the Figures 42, 43 and 44 are a series of plot of single sided pressure amplitude spectrum for each frequency. The power spectrum density is plotted at the bottom subplot for the pressure signal. The plot of power spectrum density clearly shows that the largest pressure signal contributor is at around 154 Hz. Thus, the Figure shows that with the increase in the crack depth from 4mm to 4.4mm, the power gets increased from 700 to 1900. Thus, monitoring certain key performance parameters such as static pressure, velocity flow fields help in identifying the presence of faults such as blockage and cracks in the centrifugal pump.

CHAPTER FIVE: CONCLUSIONS AND RECOMMENDATIONS

5.1 Conclusions

The fluid flow behavior inside the centrifugal pump has been studied with the help of OpenFOAM, a tool of the CFD. Both Steady-state and transient simulations were performed to study the flow pattern and the performance of the centrifugal pump.

A computational fluid domain of the centrifugal pump was modelled for which faults were incorporated and added. The CFD simulation of the centrifugal pump was performed and was compared with one of the baseline simulations.

Different faults such as blockage and presence of crack at the impeller blade are simulated to study the performance of the centrifugal pump. Blockage at the upstream of the intake pipe was modeled by decreasing the flow rate at the inlet section of the centrifugal pump. With presence of blockage at the intake of the centrifugal pump, the static pressure at the inlet region gets reduced as well as the flow discharge at the outlet gets reduced. The value of the static pressure near the inlet region gets decreased with the successive introduction of blockage at the intake of the pump which in turn increases the change in static pressure across the pump domain.

Increase in the crack depth decreases the static pressure at both the probe position. FFT has been done on the pressure signals obtained from the transient simulation of the centrifugal pump with the presence of crack in the impeller blade. The power spectrum density shows a high-power component of the pressure signal at around 154 Hz. When the crack depth is increased, the power spectrum density at this frequency gets increased.

Pump flow velocity and static pressure are major performance parameters of the centrifugal pump. Live monitoring and post-processing of the such parameter values helps in identifying the presence of faults such as blockage and crack inside the pump impellers. The deviation of these parameters from its base value indicates the occurrence of the faults in the centrifugal pump. Thus, helping in preventive maintenance and diagnostic tools for the fault detection and diagnosis system.

5.2 Recommendations

1. The present study assumed that no cavitation occurs due to blockage. But literature shows that with enough blockage at the inlet, the chance of occurrence of cavitation is high. This paper recommends considering the cavitation phenomenon for further studies.
2. Unstructured mesh is used in the simulation. The use of structured mesh results in faster convergence and accurate solution.
3. Five Symmetrical cracks are introduced as a fault in the impeller blades. However, the geometry of the cracks in real case scenario is not symmetrical as modeled in this study. Thus, irregular and unsymmetrical cracks can be introduced to model the crack for further studies.

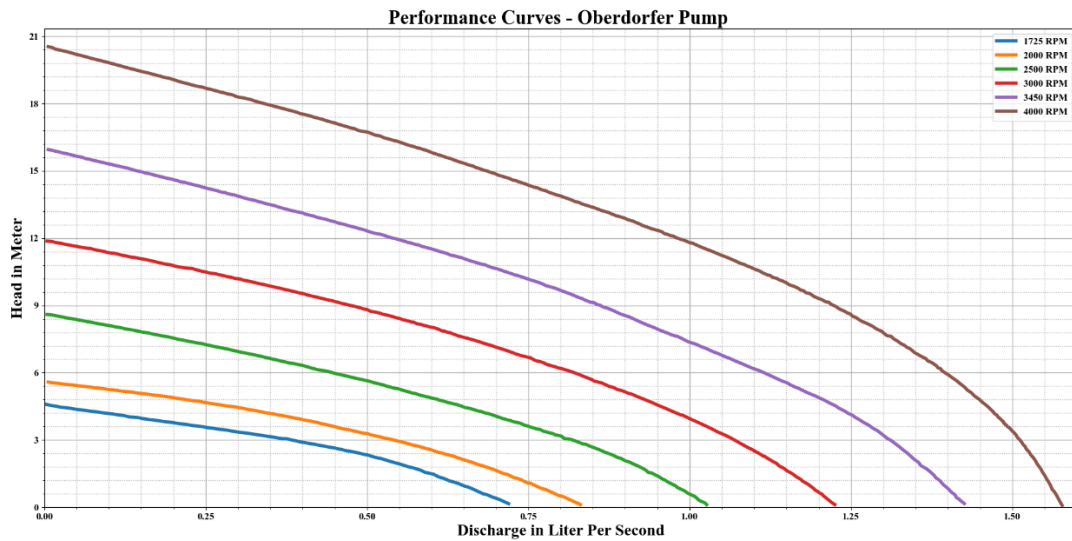
REFERENCES

1. Bhattraï, S., Baar, J. H., & Neely, A. J. (2018). Efficient uncertainty quantification for a hypersonic trailing-edge flap, using gradient-enhanced kriging. *Aerospace Science and Technology*, 80, 261-268. doi:<https://doi.org/10.1016/j.ast.2018.06.036>
2. Caruso, F., & Maskell, C. (2019). *Effect of the axial gap on the energy consumption of a single-blade wastewater pump*.
3. Huang, S., Wei, Y., Guo, C., & Kang, W. (2019). Numerical Simulation and Performance Prediction of Centrifugal Pump's Full Flow Field Based on OpenFOAM. *Processes*. doi:<http://dx.doi.org/10.3390/pr7090605>
4. Jaiswal, N. P. (2014). CFD Analysis of Centrifugal Pump: A Review. *Journal of Engineering Research and Applications*, 178-178.
5. Kumar, D., Dewangan, A., Tiwari, R., & Bordoloi, D. (2021). Identification of inlet pipe blockage level in centrifugal pump over a range of speeds by deep learning algorithm using multi-source data. *Measurements*. doi:<https://doi.org/10.1016/j.measurement.2021.110146>
6. Lei, T., Baoshan, Z., Shuliang, C., Hao, B., & Yuming, W. (2013). Influence of Blade Wrap Angle on Centrifugal Pump Performance by Numerical and Experimental Study. *CHINESE JOURNAL OF MECHANICAL ENGINEERING*, 171-177.
7. Maric, T., Hopken, J., & Mooney, G. K. (2021). *The OpenFOAM Technology Primer*.
8. McKee, K. K., G. F., Mazhar, I., Entwistle, R., & Howard, I. (2011). *A review of major centrifugal pump failure modes with application to the water supply and sewerage industries*.
9. Mohanty, A. R., Pradhan, P. K., Mahalik, N. P., & Dastidar, S. G. (2012). Fault detection in a centrifugal pump using vibration. *International Journal of Automation and Control*, 261-276.
10. Rapur, J. S., & Tiwari, R. (2016). Experimental Time-Domain Vibration Based Fault Diagnosis of Centrifugal Pumps Using Support Vector Machine. *ASCE-ASME Journal of Risk and Uncertainty in Engineering Systems*.

11. Rapur, J. S., & Tiwari, R. (2019). Experimental fault diagnosis for known and unseen operating conditions of centrifugal pumps using MSVM and WPT based analyses. *Measurement*, 147. doi:<https://doi.org/10.1016/j.measurement.2019.07.037>
12. Sakthivel, N., Sugumaran, V., & Babudevasenapati, S. (2009). Vibration based fault diagnosis of monoblock centrifugal pump using decision tree. *Expert Systems with Applications*, 4040-4049. doi:<http://dx.doi.org/10.1016/j.eswa.2009.10.002>
13. Shah, S. R., Jain, S. V., Patel, R. N., & Lakhera, V. J. (2013). CFD for centrifugal pumps: a review of the state of the art. *Procedia Engineering* (pp. 715-720). Elsevier Ltd.
14. Singh, D., Suhane, D. A., & Thakur, M. K. (2015). The study of Failure Analysis of Centrifugal Pump on the Basis of Survey. *International Journal of Science and Research (IJSR)*.
15. Smith, D. A. (2016). *Modelling Cavitation in Centrifugal Pumps Using OpenFOAM*.
16. Tiwari, R., Bordoloi, D., & Dewangan, A. (2020). Blockage and cavitation detection in centrifugal pumps from dynamic pressure signal using deep learning algorithm. *Measurements*. doi:<https://doi.org/10.1016/j.measurement.2020.108676>
17. Versteeg, H. K., & Malalasekera, W. (1995). *An Introduction to Computational Fluid Dynamics*. Pearson Education Limited.
18. Xie, S. (2010). *Studies of the ERCOFTAC Centrifugal Pump with OpenFOAM*.
19. Yannopoulos, S. I., Lyberatos, G., Theodossiou, N., Li, W., Valipour, M., Tamburrino, A., & Angelakis, A. N. (2015). Evolution of Water Lifting Devices (Pumps) over the Centuries Worldwide. *Water*, 5031-5060. doi:<https://doi.org/10.3390/w7095031>

APPENDIX

1. Pump Performance Chart Oberdorfer 60P



2. MRFPProperties

While performing the steady-state simulations using the Frozen-Rotor approach, the MRFPProperties is used. This Dictionary creates a MRF zone which is the rotating component of the turbomachinery. This file helps in creating a rotating reference frame for the simulation. In the simulation, the impeller rotor is set as a MRF zone. The code for the MRFPProperties is shown below:

```
MRF1
{
    cellZone    rotor;
    active      yes;

    // Fixed patches (by default they 'move' with the MRF zone)
    nonRotatingPatches (ami1_2 ami3_2 ami1_1 ami3_1);

    origin      (0 0 0);
    axis        (1 0 0);
    omega       188.49555921538757;
}
```

3. dynamicMeshDict

While performing the transient simulation with the Sliding-Mesh approach, the file dynamicMeshDict is used. The file creates a dynamic mesh of the impeller rotor cellzone and motion function is activated using rotatingMotion keyword.

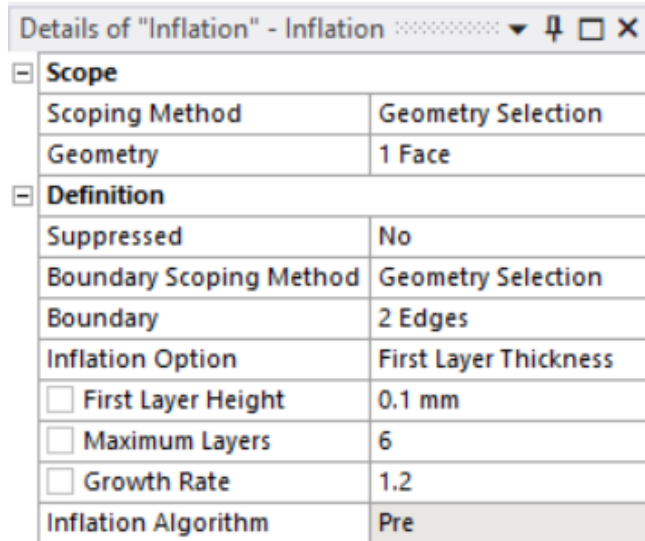
The code for the dynamicMeshDict is shown below:

```

dynamicFvMesh dynamicMotionSolverFvMesh;
motionSolverLibs ( "libfvMotionSolvers.so" );
motionSolver solidBody;
cellZone rotor;
solidBodyMotionFunction rotatingMotion;
origin (0 0 0);
axis (1 0 0);
omega 314.159;

```

4. Details of Inflation Layer used in the Inlet Domain



5. Grid Independence Test Data

The following table contains the data used to generate the grid independence test plot shown in Figure 20.

Numer of Mesh Element	Head Obtained (m)	Force (N)	Torque (Nm)
67170	2.98	71.29	0.2468
140252	3.0304	71.72	0.25004
203493	3.03337	73.098	0.24699
279231	3.0288	73.17	0.2472
302241	3.03417737	73.43	0.2452
331679	3.05386	74.28	0.2405
360053	3.056598	74.57	0.2384
402704	3.059319	74.2	0.2412



त्रिभुवन विश्वविद्यालय
Tribhuvan University
इन्जिनियरिङ अध्ययन संस्थान
Institute of Engineering

डीनको कार्यालय OFFICE OF THE DEAN

GPO box- 1915, Pulchowk, Lalitpur
Tel: 977-5-521531, Fax: 977-5-525830
dean@ioe.edu.np, www.ioe.edu.np
गोश्वारा पो. व. न- १९१५, पुल्चोक, ललितपुर
फोन- ५५२१५३१, फ्याक्स- ५५२५८३०

Date: November 26, 2023

To Whom It May Concern:

This is to certify that the paper titled "**Study of the Effects of Blockage in Centrifugal Pump using CFD Simulation**" (Submission# 806) submitted by **Bibek Adhikari** as the first author has been accepted after the peer-review process for presentation in the 14th IOE Graduate Conference being held during Nov 29 to Dec 1, 2023. Kindly note that the publication of the conference proceedings is still underway and hence inclusion of the accepted manuscript in the conference proceedings is contingent upon the author's presence for presentation during the conference and timely response to further edits during the publication process.

Bhim Kumar Dahal, PhD
Convener,
14th IOE Graduate Conference

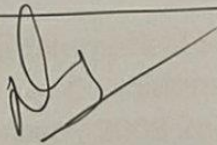


centrifugal pump flow

ORIGINALITY REPORT

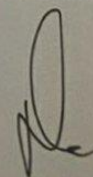
6%

SIMILARITY INDEX



PRIMARY SOURCES

- 1 publications.lib.chalmers.se
Internet 48 words — < 1%
- 2 S.R. Shah, S.V. Jain, R.N. Patel, V.J. Lakhera. "CFD for Centrifugal Pumps: A Review of the State-of-the-Art", Procedia Engineering, 2013
Crossref 43 words — < 1%
- 3 Long Meng, Meng Liu, Lingjiu Zhou, Wanpeng Wang, Cuilin Liao, Lice Zhao, Tiejou Li. "Coupling simulation of the fast startup of a centrifugal pump with cavitation in a closed-loop pipeline system", Engineering Computations, 2018
Crossref 41 words — < 1%
- 4 Fadzil Noor Gonawan. "Immobilized β -Galactosidase-Mediated Conversion of Lactose: Process, Kinetics and Modeling Studies", Springer Science and Business Media LLC, 2019
Crossref 37 words — < 1%
- 5 coek.info
Internet 32 words — < 1%
- 6 researchrepository.wvu.edu
Internet 30 words — < 1%
- 7 "Design of Piezo Inkjet Print Heads", Wiley, 2018
Crossref



centrifugal pump flow

ORIGINALITY REPORT

6%

SIMILARITY INDEX

PRIMARY SOURCES

- 1** publications.lib.chalmers.se 48 words — < 1%
Internet
- 2** S.R. Shah, S.V. Jain, R.N. Patel, V.J. Lakhera. "CFD for Centrifugal Pumps: A Review of the State-of-the-Art", *Procedia Engineering*, 2013 43 words — < 1%
Crossref
- 3** Long Meng, Meng Liu, Lingjiu Zhou, Wanpeng Wang, Cuilin Liao, Lice Zhao, Tieyou Li. "Coupling simulation of the fast startup of a centrifugal pump with cavitation in a closed-loop pipeline system", *Engineering Computations*, 2018 41 words — < 1%
Crossref
- 4** Fadzil Noor Gonawan. "Immobilized β -Galactosidase-Mediated Conversion of Lactose: Process, Kinetics and Modeling Studies", Springer Science and Business Media LLC, 2019 37 words — < 1%
Crossref
- 5** coek.info 32 words — < 1%
Internet
- 6** researchrepository.wvu.edu 30 words — < 1%
Internet
- 7** "Design of Piezo Inkjet Print Heads", Wiley, 2018
Crossref

20 words — < 1%

8 Li-Kun Huang. "Numerical Study on Air Flow with Various Accuracy Conditions in a Turbulent Contact Absorber", 2008 2nd International Conference on Bioinformatics and Biomedical Engineering, 05/2008
Crossref 19 words — < 1%

9 www.aerg.org.rw
Internet 18 words — < 1%

10 www.qucosa.de
Internet 18 words — < 1%

11 Si Huang. "Numerical simulation of 3D turbulent flow through an entire stage in a multistage centrifugal pump", International Journal of Computational Fluid Dynamics, 6/1/2006
Crossref 17 words — < 1%

12 Yue Zhang, Chenchen Song. "A Novel Design of Centrifugal Pump Impeller for Hydropower Station Management Based on Multi-Objective Inverse Optimization", Processes, 2023
Crossref 16 words — < 1%

13 dspace.plymouth.ac.uk
Internet 16 words — < 1%

14 ethos.bl.uk
Internet 14 words — < 1%

15 usermanual.wiki
Internet 14 words — < 1%

16 S. Gosavi, N. Kulkarni, C.S. Mathpati, D. Mandal. "CFD modeling to determine the minimum fluidization velocity of particles in gas-solid fluidized bed at different temperatures", Powder Technology, 2018

Crossref

13 words — < 1%

17 ethesis.inp-toulouse.fr

Internet

13 words — < 1%

18 www.electrochemsci.org

Internet

13 words — < 1%

19 Sakthivel, N.R.. "Comparison of decision tree-fuzzy and rough set-fuzzy methods for fault categorization of mono-block centrifugal pump", Mechanical Systems and Signal Processing, 201008

Crossref

12 words — < 1%

20 dk.um.si

Internet

12 words — < 1%

21 pressurewasherify.com

Internet

12 words — < 1%

22 www.diva-portal.org

Internet

12 words — < 1%

23 repository.tudelft.nl

Internet

11 words — < 1%

24 Habib, M.A.. "Evaluation of flow maldistribution in air-cooled heat exchangers", Computers and Fluids, 200903

Crossref

10 words — < 1%

25 Jiří Kozák, Pavel Rudolf, Milan Sedlář, Vladimír Habán, Martin Hudec, Rostislav Huzlík.

10 words — < 1%

"Numerical simulation and experimental visualization of the separated cavitating boundary layer over NACA2412", EPJ Web of Conferences, 2015

Crossref

26 link.springer.com 10 words — < 1%
Internet

27 Lin Wang, Chunguo An, Nini Wang, Yaming Ping, Kun Wang, Ming Gao, Suoying He. "Numerical Simulation of Axial Inflow Characteristics and Aerodynamic Noise in a Large-Scale Adjustable-Blade Fan", Fluid Dynamics & Materials Processing, 2020 9 words — < 1%
Crossref

28 Sourabh Jogee, B.V.S.S.S. Prasad, Kameswararao Anupindi. "Large-eddy simulation of non-isothermal flow over a circular cylinder", International Journal of Heat and Mass Transfer, 2020 9 words — < 1%
Crossref

29 Cornelius, Christian, Thomas Biesinger, Laith Zori, Rubens Campregher, Paul Galpin, and André Braune. "Efficient Time Resolved Multistage CFD Analysis Applied to Axial Compressors", Volume 2D Turbomachinery, 2014. 8 words — < 1%
Crossref

30 Dhiraj Kumar, Aakash Dewangan, Rajiv Tiwari, D.J. Bordoloi. "Identification of Inlet Pipe Blockage Level in Centrifugal Pump Over a Range of Speeds by Deep Learning Algorithm Using Multi-Source Data", Measurement, 2021 8 words — < 1%
Crossref

31 Nagendra Singh Ranawat, Jatin Prakash, Ankur Miglani, Pavan Kumar Kankar. "Performance 8 words — < 1%

evaluation of LSTM and Bi-LSTM using non-convolutional features for blockage detection in centrifugal pump", Engineering Applications of Artificial Intelligence, 2023

Crossref

32 Singh, A.P.. "An overall optimum design of a sector-shaped thrust bearing with continuous circumferential surface profiles", Wear, 19870601

8 words — < 1%

Crossref

33 publikationen.bibliothek.kit.edu

Internet

8 words — < 1%

34 www.cs.bham.ac.uk

Internet

8 words — < 1%

35 www.mdpi.com

Internet

8 words — < 1%

36 Atia E. Khalifa, Amro M. Al-Qutub, Rached Ben-Mansour. "Study of Pressure Fluctuations and Induced Vibration at Blade-Passing Frequencies of a Double Volute Pump", Arabian Journal for Science and Engineering, 2011

7 words — < 1%

Crossref

37 COMPEL: The International Journal for Computation and Mathematics in Electrical and Electronic Engineering, Volume 31, Issue 2 (2012-02-25)

7 words — < 1%

Publications

38 Methma M. Rajamuni, Mark C. Thompson, Kerry Hourigan. "Efficient FSI solvers for multiple-degrees-of-freedom flow-induced vibration of a rigid body", Computers & Fluids, 2020

7 words — < 1%

Crossref

39 Yongmei Zhu, Wei Guan, Weili Wang, Cunhao Dong, Jian Zhang. "Buckling performance of stiffened polymer composite cylindrical shell", Engineering Structures, 2023

7 words — < 1%

Crossref

40 Fengying Dang, Sanjida Nasreen, Feitian Zhang. "DMD-Based Background Flow Sensing for AUVs in Flow Pattern Changing Environments", IEEE Robotics and Automation Letters, 2021

6 words — < 1%

Crossref

41 Jizhong Xiao, Ali Sadegh. "Chapter 18 City-Climber: A New Generation Wall-Climbing Robots", IntechOpen, 2007

6 words — < 1%

Crossref

42 Lecture Notes in Mechanical Engineering, 2014.

6 words — < 1%

Crossref

43 Sakthivel, N.R.. "Soft computing approach to fault diagnosis of centrifugal pump", Applied Soft Computing Journal, 201205

6 words — < 1%

Crossref

EXCLUDE QUOTES ON

EXCLUDE SOURCES

< 6 WORDS

EXCLUDE BIBLIOGRAPHY ON

EXCLUDE MATCHES

OFF